# A Model for the Depositional Evolution
# of the Volcaniclastic Succession of a Pliocene Maar Volcano
# in the Styrian Basin (Austria)

By Irmina Pöschl

With 18 Figures and 20 Tables

*Steiermark*
*Pliozän*
*Maar-Vulkanismus*
*Vulkaniklastika*
*Petrographie*
*Statistik*

*Österreichische Karte 1 : 50.000*
*Blatt 192*

## Contents

*) Anschrift der Verfasserin: Mag. Irmina Pöschl, Institut für Geologie und Paläontologie, Karl-Franzens-Universität, Heinrichstraße 26, A-8010 Graz.

# Ein Modell für die Ablagerungsentwicklung der Vulkaniklastika eines pliozänen Maar-Vulkans im Steirischen Becken (Österreich)

## Zusammenfassung

Die vulkaniklastischen Ablagerungen bei Beistein/Fehring, Österreich, sind Produkte des Vulkanismus, der vor ca. 2 Millionen Jahren die tertiären Sedimente des Steirischen Beckens durchschlug. Die bei Beistein aufgeschlossene Abfolge zeigt die Reste eines Maar-Kraters und die darin abgelagerten See-Sedimente. Eine phreatomagmatische Explosion führte zur Bildung des Kraters, der tief in die tertiären Sedimente und das vulkaniklastische Material eines älteren, nordwestlich liegenden Eruptionszentrums einschneidet. Die Ablagerung einer heißen, trockenen pyroklastischen „surge" läßt vermuten, daß die Eruption in diesem Stadium von den Wechselwirkungen zwischen gemäßigten Mengen an Grundwasser und dem aufsteigendem Magma gesteuert wurde. Eine Unterbrechung der lokalen vulkanischen Aktivität ermöglichte die Ablagerung von wiederaufgearbeitetem Material auf den steilen Innenhängen des Kraters. Eine weitere Eruption führte zur Bildung einer Abfolge von nassen „surge-Ablagerungen". Während die vulkanische Aktivität im Umfeld andauerte, wurde der Krater mit See-Sedimenten gefüllt. Nach der Ablagerung von präglazialen quartären Schottern bildeten erosive Prozesse schließlich das gegenwärtige Relief heraus.

Die Verwendung von statistischen Programmen ermöglichte eine signifikante Trennung der geologisch definierten Einheiten, wobei die Unterscheidung hauptsächlich auf Unterschieden in den Schwermineral-Spektren beruht. Die Ergebnisse bestätigen das vorgestellte geologische Modell. Die aufgrund komplexer Ablagerungsprozesse komplizierten Verteilungsmuster vulkaniklastischer Gesteinskomponenten erschweren eine statistische Klassifikation der verschiedenen Einheiten auf einer Basis der Komponentenverteilung. Eine höhere Anzahl an Proben, welche ein größeres Gebiet abdecken, könnte den Einfluß störender Faktoren ausgleichen und nützliche Verteilungsstrukturen herausheben.

## Abstract

The volcaniclastic deposits at Beistein near Fehring, Austria, are fragmental products of a period of volcanism that penetrated the Tertiary sediments of the Styrian Basin about two million years ago. The sequence exposed at Beistein represents the inner crater rim of a small maar and its crater lake deposits. An initial hydromagmatic eruption led to the formation of the Beistein crater, which is cut into Tertiary sediments and overlying volcaniclastic material derived from an eruption center to the northwest of Beistein. The deposit of a hot, dry pyroclastic surge indicates, that moderate amounts of external water interacted with the ascending magma at this stage of the eruptive sequence. During a short period of quiescence, a sequence of reworked material (lahars and grain flows) was deposited on the steep inner slopes of the crater. A second explosive event produced a succession of wet surge deposits. The crater was subsequently filled with lake deposits, while volcanic activity continued at nearby eruption centers. After the deposition of a pre-glacial Quaternary pebble bed, erosional processes eventually formed the present relief.

Statistical analysis of heavy mineral distribution in the variate deposits made a significant separation of the units possible. The results confirm the initial geological model. The complexity of depositional processes and the consequently difficult interpretation of complicated distribution patterns of volcaniclastic clasts made a reasonable statistical separation of the various units based on component analysis data difficult. A wider spread of samples over a larger area and higher sample numbers may help to minimize the influence of disturbing factors on useful patterns.

## 1. Introduction

### 1.1. Physical Setting and Geology

The pyroclastic deposits near Beistein are located in the eastern part of the Styrian Tertiary Basin (West Pannonian Basin), 60 km to the southeast of Graz (46°55'N and 16°01'E; see Fig. 1).

The initial subsidence of this sedimentary basin took place about 17.5 million years ago, in the Ottnangian stage of Miocene age. Magmatism, due to the late alpidic subduction, most likely triggered the volcanic activity in the hinterland of the Alpine Carpathian orogen (FLÜGEL & NEUBAUER, 1984; HORVATH & BERCKHEMER, 1982; ROYDEN, 1988; MEISSNER & STEGENA, 1988).

Rapid subsidence and tensional tectonics formed fault systems that subdivided the Styrian Basin into distinct segments. Syn-sedimentary deposits characterize the stages of Karpatian and early Badenian (Miocene). The volcanic activity that built up trachyandesitic and trachytic shield volcanoes, which are today covered by sediments, stopped when subsidence slowed down and strong tensional tectonics came to an end. Lacustrian-fluvial sediments derived from the rising Alps to the West, followed earlier marine units in the Styrian Basin (ARIC, 1982; CLAR, 1973; FLÜGEL & NEUBAUER, 1984; HORVATH & BERCKHEMER, 1982; SCLATER et al., 1980).

At the end of Pliocene time, volcanic activity resumed giving rise to lava flows, this time of Na-rich
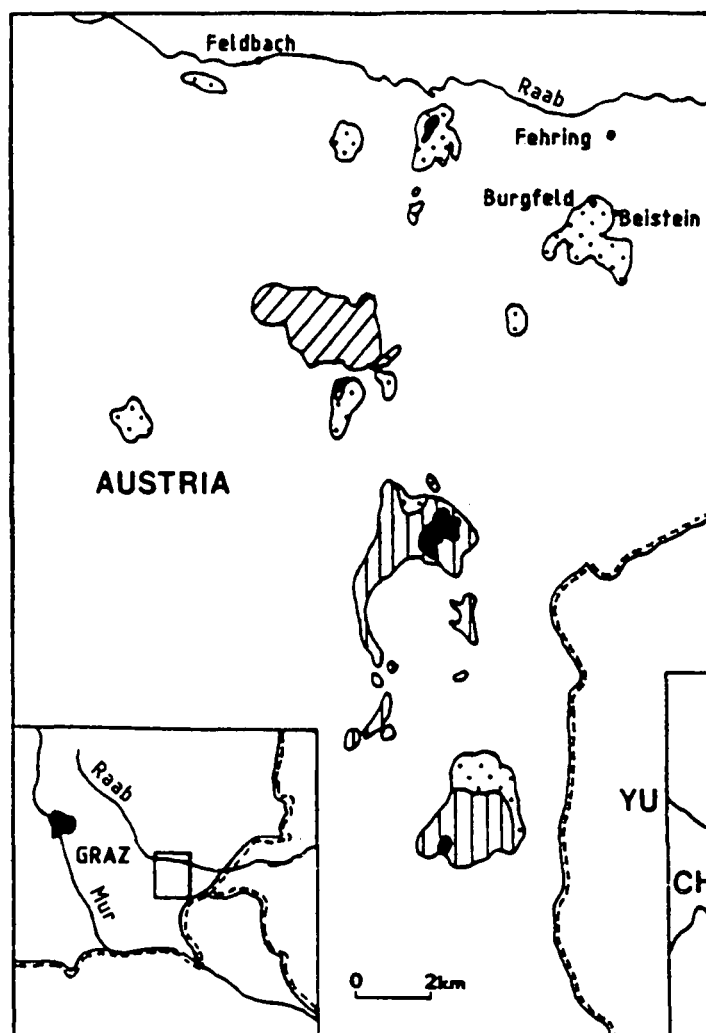
810

**Fig. 1.**
Location of volcanic and volcaniclastic deposits in the Styrian Tertiary Basin, Austria.
CS = Czechoslovakia; CH = Switzerland; D = Germany; H = Hungary; I = Italy; YU = Yugoslavia.
not patterned = Tertiary and alluvial sediments; diagonally lined = Trachyandesite & trachyte, Miocene; vertically lined = Nepheline-basanite & olivine-nephelinite, Miocene-Pliocene; stippled = Basaltic volcaniclastics; black = Postbasaltic pebbles.
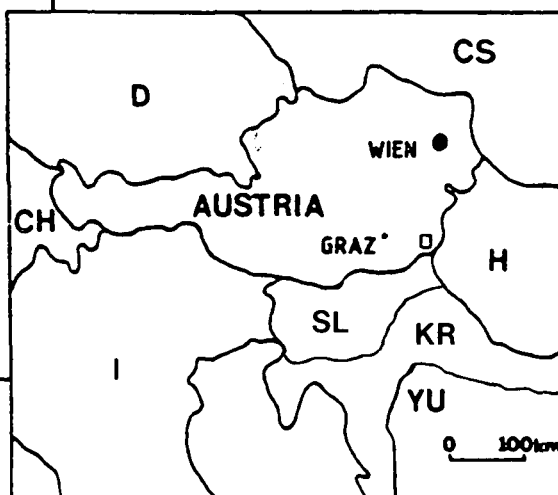
nepheline-basanitic and olivine-nephelinitic chemistry. In addition, about 40 known diatremes scattered over an area of roughly 2500 km² penetrated the Tertiary sediments. Pyroclastic deposits of this diatremes show a great amount of accidental lithics, including quartz pebbles, latites, aplites, granites and tonalites. The mineralogical composition of the ultramafic xenoliths found in pyroclastic material include spinel-lherzolites and harzburgites. They suggest equilibrium conditions of 940°–1000° Celsius and 15–27 Kb, representing an upper mantle which seems to be rather homogeneous, and lies at depths of 50–80 km (HERITSCH, 1965, 1966, 1969, 1975, 1982; HERITSCH & HÖLLER, 1970; HERITSCH & ROHANI, 1973; KURAT et al., 1976, 1977, 1980).

This volcanic activity continued into the Pannonian Basin to the east (POKA, 1988).

The only post-basaltic remnants are crater lake deposits and rare pebbly deposits, found at a few locations (EBNER & GRÄF, 1979; HÖLLER, 1982; WINKLER-HERMADEN, 1939, 1957).

## 1.2. Previous Studies

The chemistry, mineralogy and petrology of the nephiline-basanites, hauyn- and olivine-nephelinites of the Plio/Pleistocene volcanism in the Styrian Basin have been discussed by AGIORGITIS (1968, 1978), AGIORGITIS et al. (1970), ALKER et al. (1978, 1981), HERITSCH (1963, 1964, 1965, 1968 a and b, 1975, 1976

a and b), HERITSCH & HÖLLER (1970), HERITSCH & HÜLLER (1973, 1975), HÜLLER (1974), OFFENBACHER (1979), PAULITSCH (1973), POSTL & WALTER (1983), POULTIDES (1981), ROHANI (1971), SCHARBERT et al. (1981).

Papers concerning the corresponding volcaniclastic deposits (HERITSCH, 1969; HERITSCH & ROHANI, 1973; HERITSCH et al., 1960; HERMANN, 1974; HÖLLER, 1961, 1965; KURAT, 1971; KURAT et al., 1976, 1977, 1980; SCHARBERT, 1977; SCHARBERT et al., 1981;) concentrate on the interpretation of geochemical analyses of ultramafic nodules and on secondary alteration processes of the volcaniclastic material. VETTERS (1977) suggests, that the volcaniclastic sequence at Pertlstein near Fehring represents a lahar deposit.

Studies have also been carried out on the chemistry and industrial value of clay-mineral assemblages in fine-grained lake deposits at Fehring and Gnas (BERTOLDI et al., 1983; EBNER & GRÄF, 1979; HÖLLER, 1982; VOGELHUBER & WEIGEL, 1961; WIEDEN & SCHMIDT, 1956). The products of the basaltic volcanism and the late erosional processes and post-basaltic deposits were mapped and discussed by WINKLER-HERMADEN (1938, 1939, 1957).

The list of previous studies is based on text and references given in "Steiermark" (FLÜGEL & NEUBAUER,

811

1984) and on personal reading. I would like to apologize for inevitable incompleteness.

## 1.3. Objective of the Study

Several studies have been carried out on the geochemical and mineralogical aspects of the volcaniclastic successions near Fehring, Austria (see section 1.2.). However, the depositional processes and environmental conditions at the time of volcanic activity are not clearly understood.

This paper attempts to raise a number of essential questions concerning the local basaltic volcanism near Fehring:

○ What was the style of the eruptive volcanic activity that gave rise to the deposits at Beistein?

○ What were the physical and sedimentary processes involved?

○ Is there any evidence for sudden changes in the depositional history as documented by the exposed successions?

○ Will it be possible, and if so to what extent, to reconstruct the ancient environmental conditions?

There are many ways to approach these questions; the objective of this study, however, is the documentation and consideration of characteristic features within one specific volcanic succession at Beistein. This sequence is thought to be representative of the physical processes that have led to the deposition of the surrounding volcaniclastic deposits at Beistein.

Due to discontinuous outcrops, complexity of lateral facies changes and age relationships in fragmentally exposed deposits, investigations have been restricted to a small area (for detailed mapping see PÖSCHL, 1990) If restricted sets of heavy mineral data and data from component analysis (see section 2.) can provide

sufficient information for a reasonable stratigraphic and facies model, multivariate statistical methods should allow a significant separation between the visually distinguished units. The study emphasizes the reconstruction of the possible paleo-environmental, rather than spatial and paleo-geographic relationships. Correlation of the vertical sequence being studied with the units mapped in the surrounding area, may show a significant association of facies, which then could be interpreted in terms of the physical processes operating at the time of formation of the Beistein eruptive center.

## 1.4. Sample Site and the Geological Map

Because of extremely poor availability of outcrops in the field, reasonable sampling has been limited to an abandoned quarry for building stones on a hill near Beistein (see Fig. 1). The quarry cliffs, facing north and east, show a complex succession of various volcaniclastic deposits, which tend to have abrupt lateral changes (Fig. 2).

Samples were taken from two vertical cross-sections (Fig. 4) and laterally from units A, E and G (see Figs. 3 and 5).

The area surrounding the main outcrop covers about 2 km² and has been mapped at a scale of 1 : 5.000 (PÖSCHL, 1990). Areas lacking reliable outcrops have been given the signature "debris". Dashed lines represent suggested but not proven geological contacts.

Several units can be clearly distinguished:

● The underlying Tertiary sediments (Pannon) of the Styrian Basin topographically confine the volcaniclastic successions to the north and south. They also show through the volcaniclastic cover as small patches, where they have been exposed by ero-
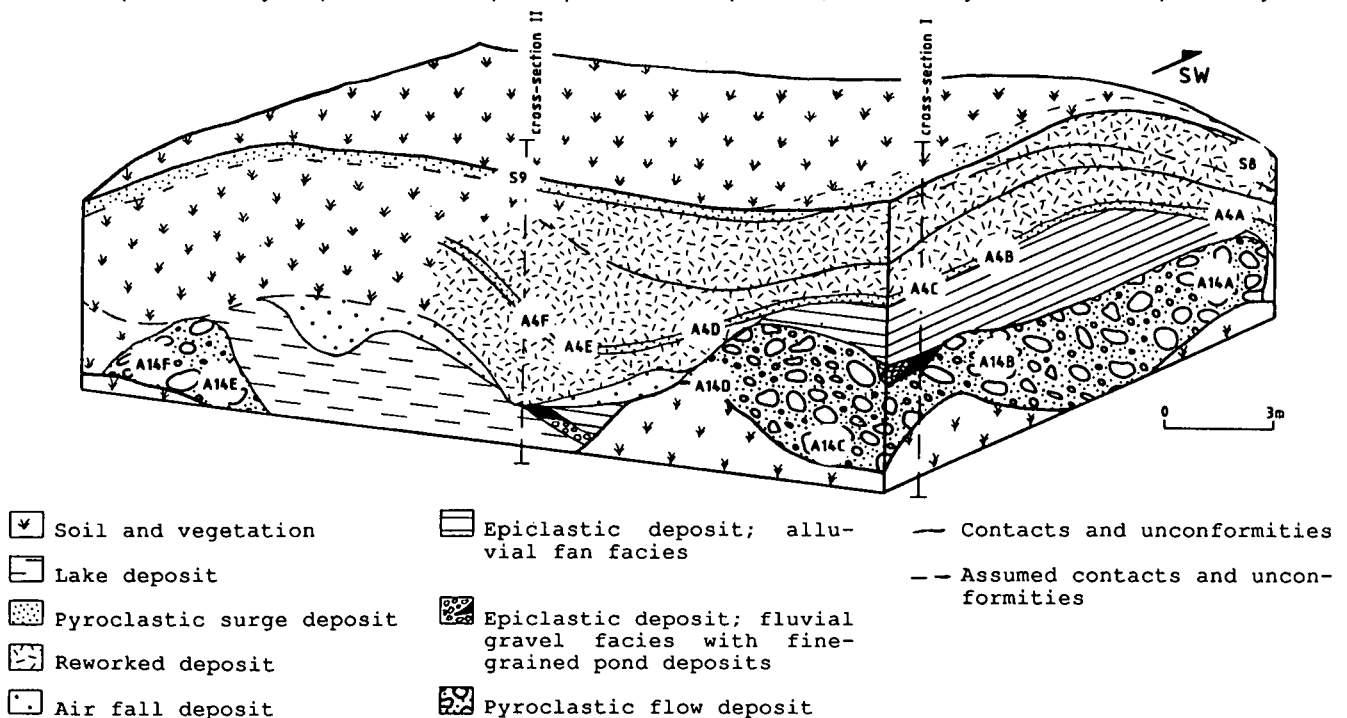


| ✔ | Soil and vegetation | | Epiclastic deposit; alluvial fan facies | | —— Contacts and unconformities |
| | Lake deposit | | | | — — Assumed contacts and unconformities |
| | Pyroclastic surge deposit | | Epiclastic deposit; fluvial gravel facies with fine-grained pond deposits | | |
| | Reworked deposit | | | | |
| | Air fall deposit | | Pyroclastic flow deposit | | |

Fig. 2.
Sketch of the volcaniclastic succession exposed at the quarry cliff near Beistein.
Sample locations: A4A to A4F = pyroclastic surge deposit I; A14A to A14F = pyroclastic flow deposit; S8, S9 = pyroclastic surge deposit II.
For further explanation see text.

Generalized
cross-section
(Fig. 4.1.)

LEGEND

| | |
|---|---|
| [.·.] | Alluvial |
| [v v] | Debris |
| [●] | Postbasaltic pebbles |
| [▒] | Epiclastic debris flow deposit |
| [≡] | Crater lake deposit |
| [▓] | Pyroclastic surge deposit |
| [⊠] | Undifferentiated volcaniclastics |
| [°°] | Tertiary sediments |

I    Cross-section  I
II   Cross-section  II

0    100   200   300   400   500m

Fig. 3.
Geological map of the area surrounding the main outcrop.

813
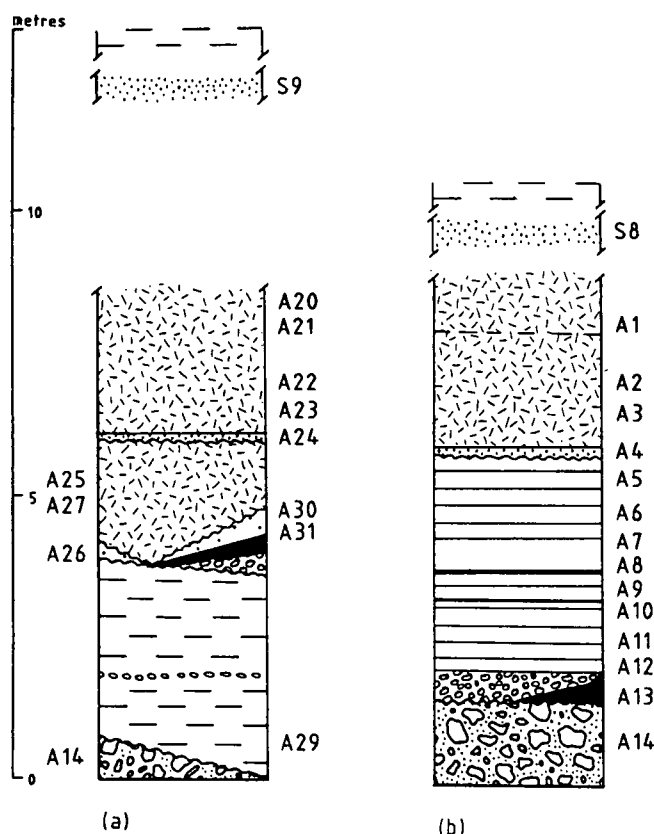
Fig. 4.
Sample locations in (a) cross-section II, (b) cross- section I.
For legend see Fig. 2.

A prominent topographic high to the west of Beistein is formed by a sequence of volcaniclastic rock with inclinations of 75° to 80°. The steep inclination is thought to be the result of secondary events, probably seismic activity or instability of the edifice, that caused parts of the crater wall to collapse forming a coarse volcanic breccia. These huge blocks are occasionally seen, but their relationship to each other and the overall geology is not understood.

At the quarry, pyroclastic flow, surge and also air fall deposits can alternate with a wide variety of epiclastic and reworked material.

One of the stratigraphically highest units in the outcrops, a succession of surge deposits, shows low-angle-cross-stratification and bomb sags. This unit can be traced around the hill describing half of a circle with beds inclined 35o to 50° towards the center (Fig. 5).

❸ If the unit described above represents the ancient crater rim, then the overlying sequence of fine grained sandy-silty beds can be interpreted as c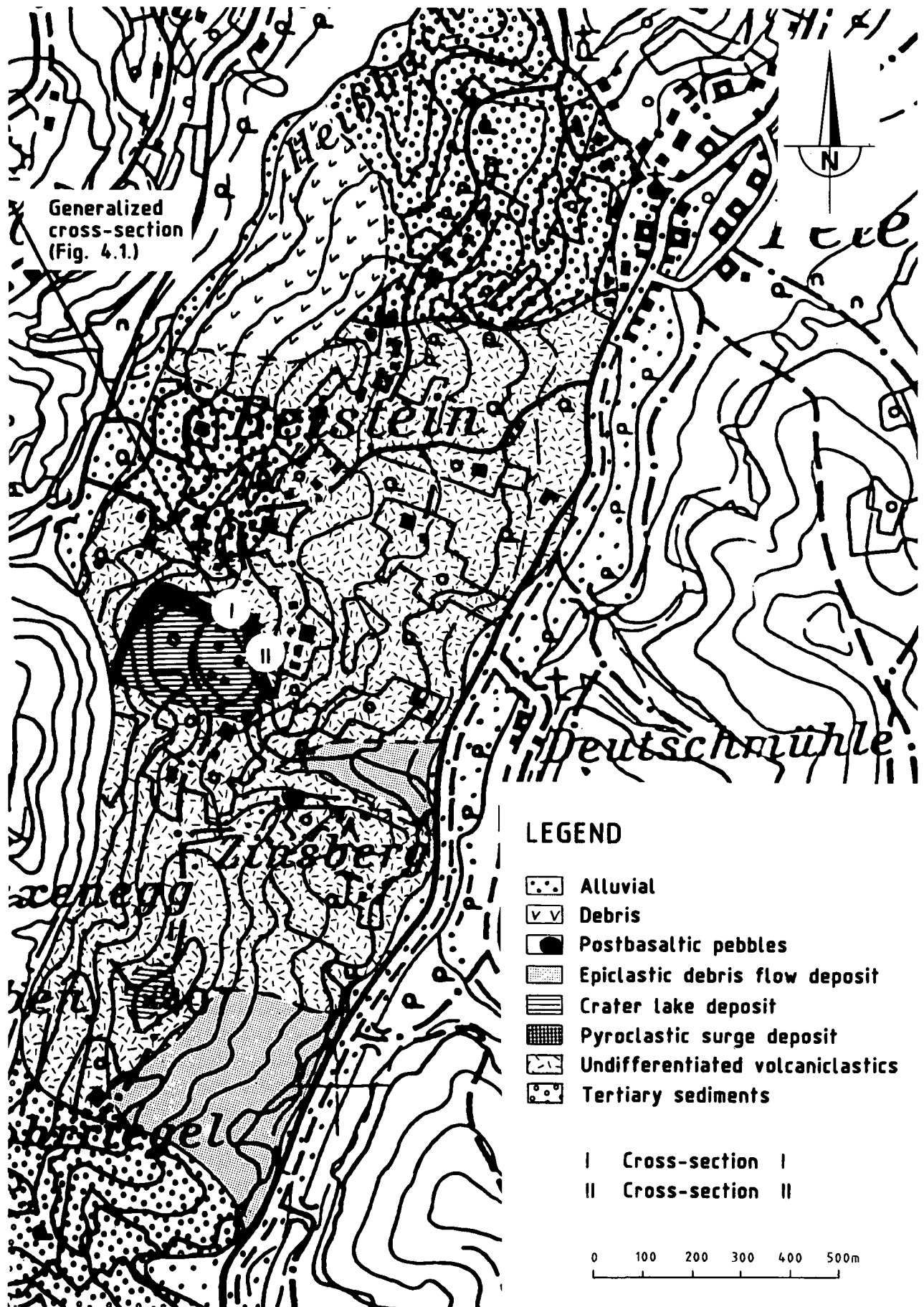rater lake deposit. Local occurrences of similar material indicate a smaller parasitic crater near Zinsberg about 1 km to the south of Beistein.
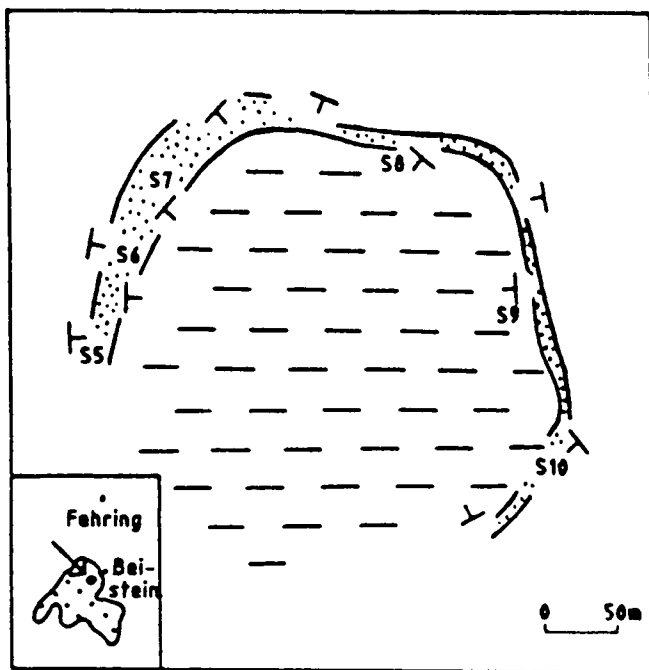


Fig. 5.
Pyroclastic surge deposits describing the ancient crater rim.
Beds show inclination toward the eruption center. S5 - S10 = sample locations; not patterned = undifferentiated volcaniclastic deposits; stippled = pyroclastic surge deposits; dashed lines = lake deposit.

sional processes. The surprisingly irregular pattern of the intersection between lithological contacts and the present topographical surface is explained as a result of the deposition of younger volcanic material on a significant pre-depositional paleo-relief. Furthermore, pyroclastic and epiclastic flows tend to accumulate in topographic depressions. This produces discontinuous deposits that are thick along the depression axis and thin out drastically towards the edges.

❷ Volcaniclastic material has been subdivided into undifferentiated volcaniclastics, epiclastic, pyroclastic and crater lake deposits (3.). Undifferentiated volcaniclastics include deposits that lack characteristic features allowing for a specific classification (e.g. reworked material, etc.). The term epiclastic is used for those deposits that contain fragments of consolidated pyroclastic rock (FISHER & SCHMINCKE, 1984).

Classified epiclastic units at Beistein are thought to represent volcaniclastic debris flow and grain flow deposits (Fig. 3). This classification is based on the assumed depositional surface and characteristic features such as high content of fine matrix, subangular to rounded clasts of pyroclastic rock in an open framework, and poor sorting. The deposits may have formed as the near-source facies (FISHER & SCHMINCKE, 1984; also see section 4.2.) of the small eruptive center at Beistein. Because of the lack of definite evidence of original contacts, the epiclastic deposits have been drawn schematically as fans (Fig. 3).

Similar to the succession at Beistein, the lake deposit at Burgfeld, near Fehring (Fig. 1), is also surrounded by a marginal circle of volcaniclastic material, underlain by Tertiary sediments (EBNER & GRÄF, 1979; FLÜGEL & HERITSCH, 1968). According to the geological and spatial setting, the sequence at Fehring is interpreted as a Pliocene "maar". Although the genetic history and stratigraphy of the approximately 1000 m wide crater is not known in detail (FLÜGEL & HERITSCH, 1968), it is thought to be genetically closely related to the succession at Beistein (see chapter 4.; Fig. 15).

❹ A restricted layer (outcropping over an area of approximately 10 m²) of post-basaltic pebbles ("Post-basaltische Schotter") near Zinsberg lies stratigraphically on top of volcaniclastic material. Presumably this pebble bed is of Early Quaternary pre-glacial age (FLÜGEL & NEUBAUER, 1984; WINKLER-HERMADEN, 1957) and represents the final sequence of sediments deposited in the Styrian Basin.

# 2. Instrumentation and Methods of Data Collection

## 2.1. Grainsize Analysis

Wet mechanical analysis was used as a data source for examining the grainsize distribution and variation within the unconsolidated deposits (A2, A6H–A13). A5 of the lower epiclastic unit, A1 and A3 of the upper unit as well as all pyroclastic deposits were unsuited for sieving analysis due to their level of consolidation.

The analyses were made with a set of sieves with mesh sizes spaced at one-$\Phi$ intervals ($\Phi = -\log_2 d$, d being the grainsize in millimeters), ranging from -4 to +4 $\Phi$. Cumulative curves of the grainsize distributions were constructed on arithmetic probability paper. The Inman parameters (median diameter (Md) and graphical standard deviation (Sigma) as a measure of sorting) were determined, using the formulae developed by INMAN (1952):

$$Md(\Phi) = (\Phi)50$$
$$Sigma(\Phi) = ((\Phi)84-(\Phi)16)/2$$

## 2.2. Heavy Mineral Analysis

In order to obtain the required grain fraction of the volcaniclastic material (0.05 mm < diameter < 0.4 mm), the samples were crushed and sieved. Na-Polywolframat-solution (specific density = 2.95 g/cm) was used for the heavy liquid separation, and grain mounts were made with Permount (n = 1.54).

Data (Tab. 1 and 2.) was obtained by identifying and counting approximately 300 transparent crystal grains per slide on several area strips (wandering field of view), converted into "grain percent" (100 %). The proportion of opaque minerals is expressed as grain percentage (opaque + transparent minerals = 100 %). Those minerals that do not exceed 2 grain percent are listed under "others", including spinel, rutile, zircon, anatase. The following minerals were identified and counted seperately: olivine, hornblende, pyroxene and garnet.

An occasionally large discrepancy between mineralogical abundances (olivine, hornblende), which were determined by heavy mineral analysis and component analysis in thin sections, respectively, may be due to the presence of ultramafic xenoliths and xenocrysts. Ultramafic nodules and big basaltic hornblende crystals are easily missed when cutting the rocks for the preparation of thin sections. However, the occurrence of one small fragment in crushed material, used for the heavy mineral separation, may be enough to significantly raise the value for a certain fraction. Orthopyroxenes, which are not normative in alkaline basalts but may be found in the heavy mineral spectra of some samples, are also derived from ultramafic xenoliths. Since the heavy mineral analysis is sup-

| S.No. | ol | hb | py | gr | ot | op | wt%HM |
|---|---|---|---|---|---|---|---|
| profile I | | | | | | | |
| A1 | 34.2 | 32.0 | 24.3 | 8.5 | 1.0 | 12.5 | 2.3 |
| A2 | 57.2 | 31.9 | 8.3 | 1.7 | 0.9 | 3.2 | 6.7 |
| A3 | 62.8 | 21.4 | 10.8 | 3.2 | 1.8 | 7.5 | 6.1 |
| A4C | 44.8 | 7.7 | 39.4 | 6.4 | 1.7 | 9.1 | 3.4 |
| A5 | 70.5 | 12.0 | 15.2 | 1.3 | 1.0 | 8.6 | 11.3 |
| A6H | 75.1 | 7.5 | 4.2 | 11.5 | 1.7 | 7.9 | 17.3 |
| A6L | 71.4 | 15.3 | 2.1 | 7.7 | 3.5 | 8.6 | 17.6 |
| A7 | 62.6 | 20.0 | 12.0 | 2.8 | 2.6 | 7.2 | 14.0 |
| A8 | 60.0 | 19.1 | 12.3 | 6.0 | 2.6 | 19.8 | 5.0 |
| A9H | 66.6 | 13.4 | 10.6 | 7.1 | 2.3 | 12.5 | 6.3 |
| A9L | 73.0 | 13.9 | 3.9 | 7.9 | 1.3 | 7.9 | 9.6 |
| A10 | 72.4 | 10.9 | 8.3 | 7.2 | 1.2 | 9.8 | 10.3 |
| A11 | 77.7 | 9.1 | 7.5 | 3.6 | 2.1 | 7.2 | 15.7 |
| A12/4 | 71.6 | 9.1 | 4.9 | 7.2 | 7.2 | 17.9 | 12.3 |
| A12/3 | 75.0 | 11.9 | 7.2 | 4.4 | 1.5 | 5.5 | 18.9 |
| A12/2 | 74.9 | 10.6 | 8.6 | 5.2 | 0.7 | 8.5 | 14.2 |
| A12/1 | 67.8 | 8.6 | 6.7 | 10.4 | 6.5 | 8.0 | 12.7 |
| A13 | 67.1 | 10.6 | 8.0 | 9.9 | 4.4 | 21.5 | 3.9 |
| A14B | 75.3 | 1.7 | 14.0 | 1.7 | 7.3 | 11.0 | 10.9 |
| profile II | | | | | | | |
| A20 | 62.0 | 21.8 | 9.3 | 6.3 | 0.6 | 8.5 | 7.8 |
| A21 | 47.1 | 33.5 | 12.0 | 6.5 | 1.0 | 7.2 | 7.1 |
| A22 | 55.1 | 23.0 | 15.8 | 5.5 | 0.6 | 7.5 | 4.5 |
| A23 | 53.6 | 27.0 | 12.5 | 6.6 | 0.3 | 5.9 | 5.2 |
| A24 | 41.1 | 7.3 | 44.9 | 5.1 | 1.6 | 6.0 | 4.2 |
| A25/1 | 47.5 | 16.2 | 26.2 | 8.2 | 1.9 | 7.3 | 7.3 |
| A25/2 | 50.2 | 11.6 | 31.7 | 4.0 | 2.5 | 5.9 | 5.9 |
| A26 | 49.8 | 24.5 | 18.9 | 5.2 | 1.6 | 4.2 | 9.6 |
| A27 | 60.0 | 22.0 | 12.5 | 3.1 | 2.1 | 5.8 | 7.8 |
| A30 | 46.6 | 35.0 | 10.5 | 5.5 | 2.4 | 6.0 | 10.4 |
| A31 | 59.8 | 21.5 | 11.1 | 6.4 | 1.2 | 6.0 | 9.9 |
| A29 | 61.6 | 9.2 | 15.0 | 10.8 | 3.4 | 7.3 | 8.3 |
| A14E | 71.1 | 7.9 | 11.6 | 6.3 | 3.1 | 14.5 | 7.8 |

Table 1.
Data derived from heavy mineral analysis, cross-section I and cross-section II (32 samples).
Values represent percent of grain counts (ol, hb, py, ot, op) and weight percent (wt %HM) (see chapter 2.2.).
S.No. = sample number; ol = olivine; hb = hornblende; py = pyroxene; gr = garnet; ot = others; op = opaques; wt%HM = total weight percent of heavy minerals per sample.

| S.No. | ol | hb | py | gr | ot | op | wt%HM |
|---|---|---|---|---|---|---|---|
| **unit A14** | | | | | | | |
| A14A | 82.5 | 0.8 | 13.6 | 0.6 | 2.5 | 14.6 | 12.2 |
| A14B | 75.3 | 1.7 | 14.0 | 1.7 | 7.3 | 11.0 | 10.9 |
| A14C | 73.0 | 3.4 | 14.3 | 2.3 | 7.0 | 9.9 | 13.3 |
| A14C1 | 72.1 | 4.2 | 12.6 | 5.0 | 6.1 | 14.3 | 13.2 |
| A14D | 73.6 | 6.0 | 15.5 | 1.0 | 3.9 | 12.8 | 8.3 |
| A14E | 71.1 | 7.9 | 11.6 | 6.3 | 3.1 | 14.5 | 7.8 |
| A14F | 77.1 | 4.0 | 13.0 | 2.3 | 3.6 | 9.1 | 9.8 |
| **unit A4** | | | | | | | |
| A4A | 58.9 | 7.5 | 28.8 | 4.5 | 0.3 | 7.2 | 8.2 |
| A4B | 44.7 | 12.7 | 35.3 | 6.0 | 1.3 | 8.0 | 6.4 |
| A4C | 44.8 | 7.7 | 39.4 | 6.4 | 1.7 | 9.1 | 3.4 |
| A4D | 34.3 | 10.5 | 48.1 | 6.5 | 0.6 | 6.4 | 2.5 |
| A4E | 39.8 | 10.9 | 39.2 | 8.1 | 2.0 | 9.1 | 3.1 |
| A4F | 41.1 | 7.3 | 44.9 | 5.1 | 1.6 | 23.7 | 1.9 |
| **unit S** | | | | | | | |
| S5 | 18.8 | 32.3 | 44.7 | 3.3 | 0.9 | 6.0 | 8.9 |
| S6 | 38.5 | 25.0 | 33.3 | 2.3 | 0.9 | 2.5 | 6.4 |
| S7 | 59.6 | 21.0 | 15.7 | 1.2 | 2.5 | 3.3 | 11.5 |
| S8 | 20.5 | 16.0 | 53.1 | 8.8 | 1.6 | 6.9 | 5.8 |
| S9 | 25.6 | 15.4 | 47.9 | 8.9 | 2.2 | 5.7 | 4.8 |
| S10 | 26.9 | 15.0 | 56.5 | 1.1 | 0.5 | 4.1 | 4.3 |

Table 2.
Data derived from heavy mineral analysis, layers A14, A4 and S (units A, E, G, 19 samples).
Values represent percent of grain counts (ol, hb, py, gr, ot, op) and weight percent (wt%HM) (see chapter 2.2).
For definitions see Tab. 1.

posed to represent a bulk composition, restricted to specific minerals, the grains derived from xenoliths do not falsify the obtained data. The awareness of this fact may, of course, be important for interpreting the data set.

## 2.3. Component Analysis

Using an automatic point-counter, 300 components (described below) per thin section have been examined and classified. Thin sections were made only of those samples that were consolidated enough to be cut properly. Included are all samples of the pyroclastic flow deposit (A14), the pyroclastic surge deposits (S5–S10), cross-section II (A20–A31, except A24) and A1 to A5 of cross-section I.

Components were subdivided into the following classes:

○ Matrix
○ Cryptocrystalline basaltic clasts

Table 3.
Data derived from component analysis (28 samples).
S.No. = sample number; mat = matrix; cry = cryptocrystalline basaltic clasts; vit = vitric basaltic clasts; cr = crystals; qu = quartz and feldspar clasts; ccl = clastic lithics; vol = volcanic lithics; acc = accretionary and armored lapilli; ves = vesicles.

| S.No. | mat | cry | vit | cr | qu | cll | vol | acc | ves |
|---|---|---|---|---|---|---|---|---|---|
| **profile I** | | | | | | | | | |
| A1 | 34.3 | 19.1 | 9.7 | 1.1 | 30.0 | 2.2 | 3.6 | 0.0 | 7.6 |
| A2 | 9.7 | 51.9 | 4.7 | 2.6 | 25.1 | 4.3 | 1.7 | 0.0 | 21.7 |
| A3 | 44.6 | 25.8 | 8.4 | 1.7 | 16.0 | 3.5 | 0.0 | 0.0 | 4.3 |
| A4C | 55.4 | 17.9 | 5.7 | 1.7 | 19.3 | 0.0 | 0.0 | 0.0 | 1.3 |
| A5 | 4.2 | 45.4 | 6.3 | 7.1 | 32.4 | 3.8 | 0.8 | 0.0 | 20.6 |
| **profile II** | | | | | | | | | |
| A20 | 59.8 | 18.5 | 3.7 | 1.4 | 16.6 | 0.0 | 0.0 | 0.0 | 1.3 |
| A21 | 44.6 | 23.5 | 11.8 | 1.0 | 19.1 | 0.0 | 0.0 | 0.0 | 3.7 |
| A22 | 47.8 | 23.7 | 7.1 | 0.7 | 20.7 | 0.0 | 0.0 | 0.0 | 1.7 |
| A23 | 43.9 | 27.4 | 11.5 | 2.0 | 15.2 | 0.0 | 0.0 | 0.0 | 1.3 |
| A25 | 62.2 | 16.1 | 2.3 | 0.7 | 18.7 | 0.0 | 0.0 | 0.0 | 0.3 |
| A26 | 50.3 | 28.9 | 5.4 | 0.7 | 14.0 | 0.0 | 0.0 | 0.7 | 2.0 |
| A27 | 51.7 | 24.2 | 6.5 | 2.0 | 15.3 | 0.3 | 0.0 | 0.0 | 2.0 |
| A30 | 52.7 | 17.2 | 8.8 | 2.7 | 18.6 | 0.0 | 0.0 | 0.0 | 1.3 |
| A31 | 39.6 | 28.2 | 5.4 | 2.5 | 21.4 | 0.0 | 0.0 | 2.9 | 6.7 |
| A29 | 35.9 | 21.7 | 4.8 | 2.1 | 31.4 | 4.1 | 0.0 | 0.0 | 3.3 |
| A14 | 41.6 | 27.4 | 9.8 | 4.7 | 15.2 | 0.0 | 1.3 | 0.0 | 1.3 |
| **unit 14A** | | | | | | | | | |
| A14A | 52.4 | 17.6 | 9.5 | 3.3 | 17.2 | 0.0 | 0.0 | 0.0 | 1.3 |
| A14B | 49.2 | 17.5 | 8.4 | 3.0 | 21.6 | 0.0 | 0.3 | 0.0 | 1.0 |
| A14C | 52.4 | 16.7 | 5.4 | 5.4 | 19.1 | 0.7 | 0.3 | 0.0 | 2.0 |
| A14C1 | 58.1 | 16.9 | 7.1 | 1.7 | 15.5 | 0.7 | 0.0 | 0.0 | 1.3 |
| A14D | 48.1 | 20.6 | 5.2 | 4.1 | 20.3 | 0.7 | 1.0 | 0.0 | 3.0 |
| A14E | 41.6 | 27.4 | 9.8 | 4.7 | 15.2 | 0.0 | 1.3 | 0.0 | 1.3 |
| A14F | 42.8 | 22.9 | 13.8 | 2.4 | 17.1 | 0.7 | 0.3 | 0.0 | 1.0 |
| **unit S** | | | | | | | | | |
| S5 | 38.4 | 18.3 | 22.7 | 3.0 | 17.0 | 0.3 | 0.0 | 0.3 | 0.0 |
| S6 | 30.5 | 36.6 | 10.3 | 2.1 | 19.5 | 0.3 | 0.0 | 0.7 | 2.6 |
| S7 | 40.9 | 22.3 | 19.6 | 1.7 | 14.8 | 0.7 | 0.0 | 0.0 | 1.3 |
| S8 | 45.7 | 17.1 | 5.1 | 2.7 | 28.7 | 0.0 | 0.0 | 0.7 | 2.3 |
| S9 | 40.6 | 33.5 | 3.4 | 1.0 | 18.4 | 0.0 | 0.0 | 3.1 | 2.3 |
| S10 | 20.2 | 35.1 | 19.7 | 3.2 | 19.4 | 0.4 | 0.0 | 2.0 | 17.3 |

O Vitric basaltic clasts
O Crystals
O Monomineralic clasts (quartz, feldspars)
O Clastic lithics
O Volcanic lithics
O Accretionary and armored lapilli
O Vesicles or air spaces
   For data see Tab. 3.

### 2.3.1. Matrix

The microcrystalline matrix consists of small fragments of broken country rock (quartz and feldspar chips) and minerals that are thought to be alteration products of the original matrix-forming glass shards. The grade and type of alteration may show significant variations throughout the succession and even within a single sample. The alterations may have been caused by primary processes during deposition (hot or cold, wet or dry emplacement, varying porosity) and/or secondary diagenetic influences (hydrothermal fluids, weathering). In pyroclastic deposits, densely packed matrix may in some cases have maintained its original glassy texture or even its optical isotropy.

### 2.3.2. Basaltic Volcanic clasts

Basaltic volcanic clasts of nepheline-basanitic chemistry show different grades of crystallization. They may be slightly inflated, dense and cryptocrystalline or vitric. The conformity of phenocrysts and rare joint occurrence of vitric and cryptocrystalline texture within one individual clast indicate, that they came from the same magma batch. Olivine, augite (Fig. 6 (a)), and nepheline form euhedral phenocrysts. Rare orthopyroxene crystals, xenocrysts in the silica-undersaturated magma that have presumably been derived from ultramafic nodules, may show augite or hornblende alteration coronas (Fig. 6 (b)). Xenolithic quartz grains, which have been occasionally incorporated into the ascending magma, usually lack alteration rims. This may point towards a fast ascent of the melt, but the reaction processes between quartz and silica-

undersaturated magma in general are not well understood. Furthermore, HERMANN (1974) described basaltic lapilli in nearby basaltic pyroclastic deposits of the same age, which show secondary alterations partially due to the incorporation of quartz grains.

Vitric fragments may be strongly oxidized and thus hard to recognize. Components were only classified as vitric if this assignment was obvious. Devitrified sideromelane fragments that maintained their glassy texture are included in this class, although strongly altered clasts may have lost their characteristics and thus could not be distinguished from the matrix.

With respect to their origin, the basaltic clasts in pyroclastic deposits may be subdivided into juvenile and cognate ejecta (CAS & WRIGHT, 1988; FISHER & SCHMINCKE, 1984). The mineralogical similarity of the basaltic components throughout the sequence, which is probably caused by a relatively invariable magmatic composition during the confined time of volcanic activity, make a distinction difficult.

The degree of volatile dissolution at the moment of eruption, the amount of external water involved, and the depositional processes may be the main causes for the varying proportions of cryptocrystalline and vitric basaltic clasts.

### 2.3.3. Crystals

Crystals that occur as independent components are essentially pyrogenic and include olivine, augite, nepheline and hornblende. Rutile, zircon, garnet and opaques, presumably derived from the underlying sediments, are rare and seldom seen in thin sections.

### 2.3.4. Lithic Fragments

Components that are not directly derived from the erupting magma show diverse characteristics. Angular quartz-grains (Fig. 7) and feldspar-grains were produced by the explosive fragmentation of sedimentary pebbles, which was caused by shallow hydrovolcanic eruptions. The monomineralic clasts may show undulatory extinction and recrystallization- or strain-tex-
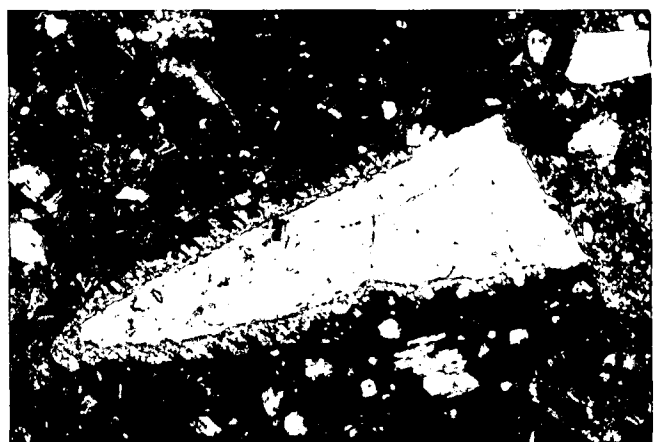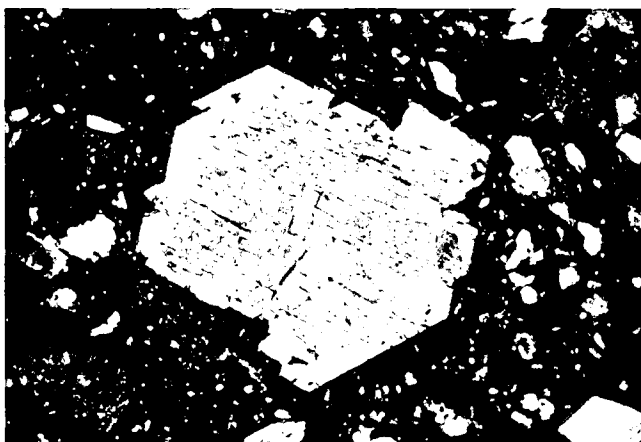




Fig. 6.
Pyrogenic crystals in basaltic clasts.
a) Clinopyroxene with marginal zoning and intergrowth lamellae in basaltic clast.
   Sample A14C, pyroclastic flow deposit, unit A.
   XPL, magnification ×26.
b) Orthopyroxene with alteration corona in basaltic clast.
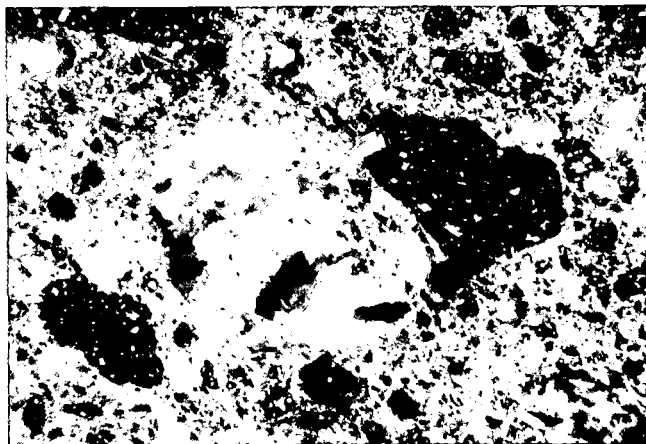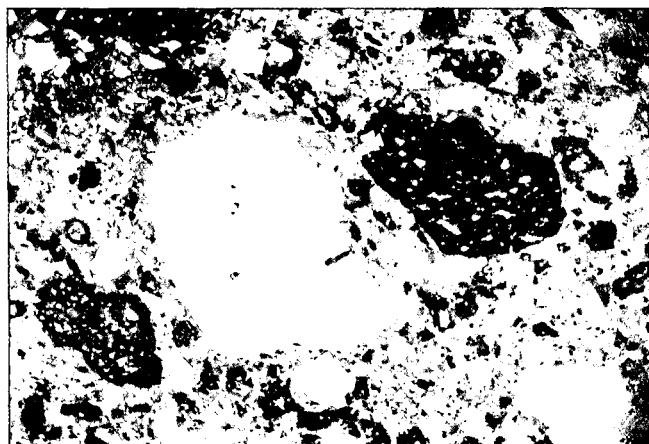   Sample A14E, pyroclastic flow deposit, unit A.
   XPL, magnification ×13.

Fig. 7.
Big lithic quartz fragment in pyroclastic flow deposit.
Sample A14B, unit A.
a) PPL.
b) XPL.
Magnification ×5.

tures due to their metamorphic history during alpidic orogeny. Small intact pebbles in epiclastic deposits may also be derived from the surrounding surficial sediments.

Clastic lithics include fragments of slightly consolidated fine-grained material of the sedimentary successions (mud or sandstone) and tuff fragments. The tuff fragments were either explosively ejected during eruptions or derived from the surface by reworking and weathering.

The rare volcanic lithics which show distinct differences in their modal mineralogy are thought to be Miocene latites that have been penetrated by the ascending basaltic magma and ejected during the eruption (FLÜGEL & NEUBAUER, 1984).

In pyroclastic deposits, lithics that are not directly derived from the erupting magma are termed accidental clasts (CAS & WRIGHT, 1988; FISHER & SCHMINCKE, 1984).

Remarkable is the lack of plutonic and metamorphic xenoliths, which are abundant at Kapfenstein and other locations.

### 2.3.5. Accretionarry Lapilli Armored Lapilli

Rare accretionary lapilli show the same microcrystalline texture as the equivalent devitrified ash matrix, but exhibit a concentric internal structure that may be obscured by secondary processes. Armored lapilli (recognizable lithic cores covered by unstructured ash) are common in some surge deposits and in the air fall deposit A31 (Fig. 8).

### 2.3.6. Vesicles

Vesiculated tuffs with entombed gas cavities are diagnostic for phreatomagmatic pyroclastic material that has been deposited under wet conditions, where ash was nearly saturated with water so that trapped air or steam could not escape (CAS & WRIGHT, 1988).

Vesicles in lahar deposits have been explained as trapped air bubbles (CRANDELL & WALDRON, 1956; CRANDELL, 1971) but may also be formed by draining away water (see section 4.5).
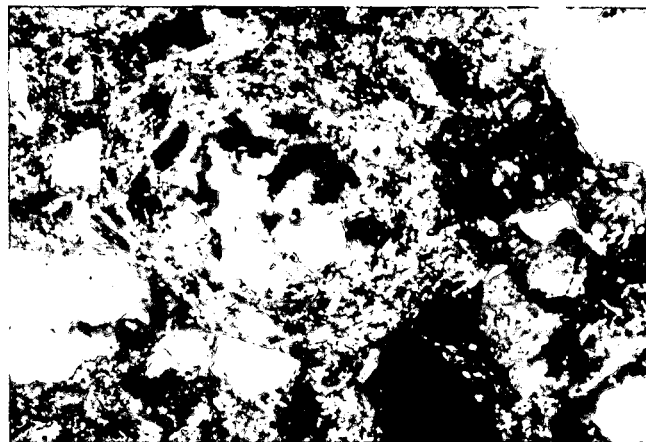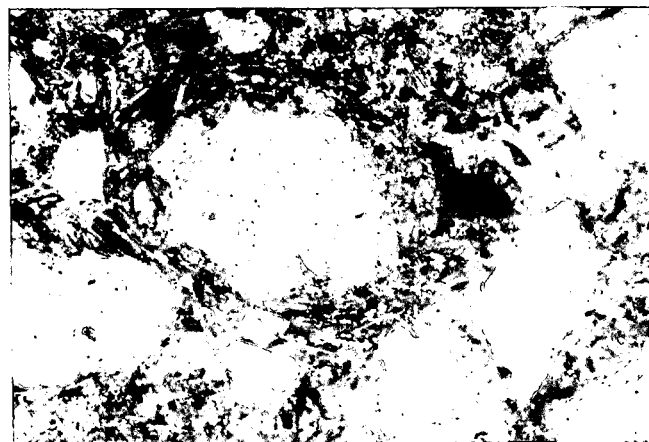


Fig. 8.
Armored lapilli with lithic core.
Sample S8, surge deposit II, unit G.
a) PPL.
b) XPL.
Magnification ×51.

Air spaces in reworked and epiclastic material may be due to draining away water and/or lack of fine-grained matrix.

### 2.3.7. Ultramafic Xenoliths

The Pliocene volcaniclastics contain a wide variety of ultramafic xenoliths (known as "Olivinbomben"). The nodules from Kapfenstein, a tuff cone to the southwest of Beistein, are derived from the upper mantle, approximately 50–80 km below surface. Modal compositions reach from lherzolite to dunite. The suite represents a residual sequence formed by different degrees of partial melting in the upper mantle (KURAT et al., 1980).

Based on heavy mineral spectra of crushed nodules and spectra of the exessively xenolith-bearing unit A (see section 3.1), the ultramafic xenoliths at Beistein may be described as dunites or dunite-lherzolites. They are rich in olivine; clino- and orthopyroxenes are less abundant, spinel and garnet are absent or rare.

It is not known, if the xenoliths at Beistein are truly derived from the upper mantle, or if they are early cummulates of the basaltic magma. Detailed analyses of the geochemistry of the material may provide further information.

The ultramafic xenoliths do not appear as a variable in the statistical component analysis, because they are easily missed and, therefore, not present in thin sections.

## 3. Description of the Deposits and their Setting

### 3.1. Pyroclastic Flow Deposit (Unit A)

The stratigraphically lowest unit of cross-section I (see Fig. 11), a pyroclastic flow deposit, is only partially exposed and its total thickness is therefore not known. A sharp contact with the overlying sediments (see section 3.2.) forms a distinct erosional unconformity.

The main components of the lowest unit are juvenile (and probably cognate) cryptocrystalline basaltic fragments, accidental clasts including a significant amount of quartz pebbles (some of them fragmented) and crystals. Basaltic fragments, mud lumps, and ultramafic nodules (see section 1.3. and Fig. 9) with basaltic crusts may be as big as 30 cm (longest dimension), though clasts of this size are rare. Clay minerals and other unidentified crystallites form a microcrystalline matrix which is thought to be an alteration product of vitric ash shards.



Fig. 10.
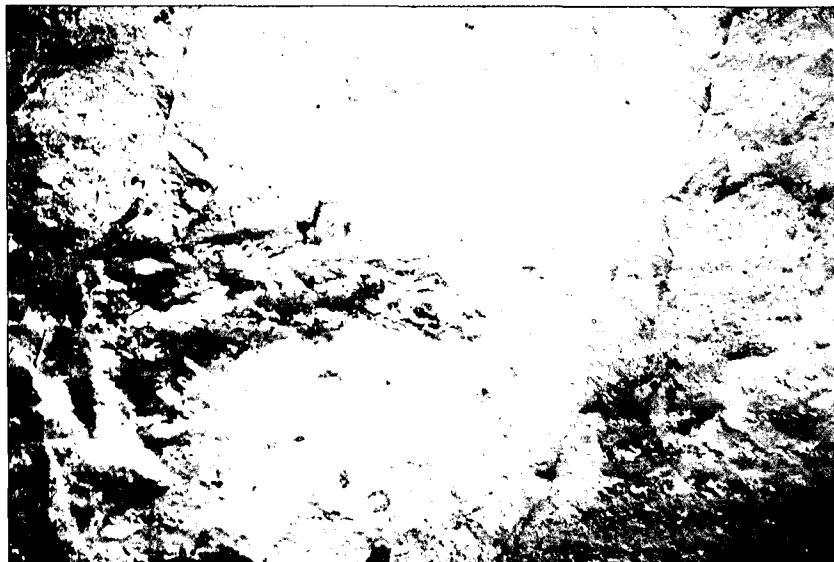Degassing pipe penetrating pyroclastic flow deposit (unit A).



Fig. 9.
Pyroclastic flow deposit (unit A).
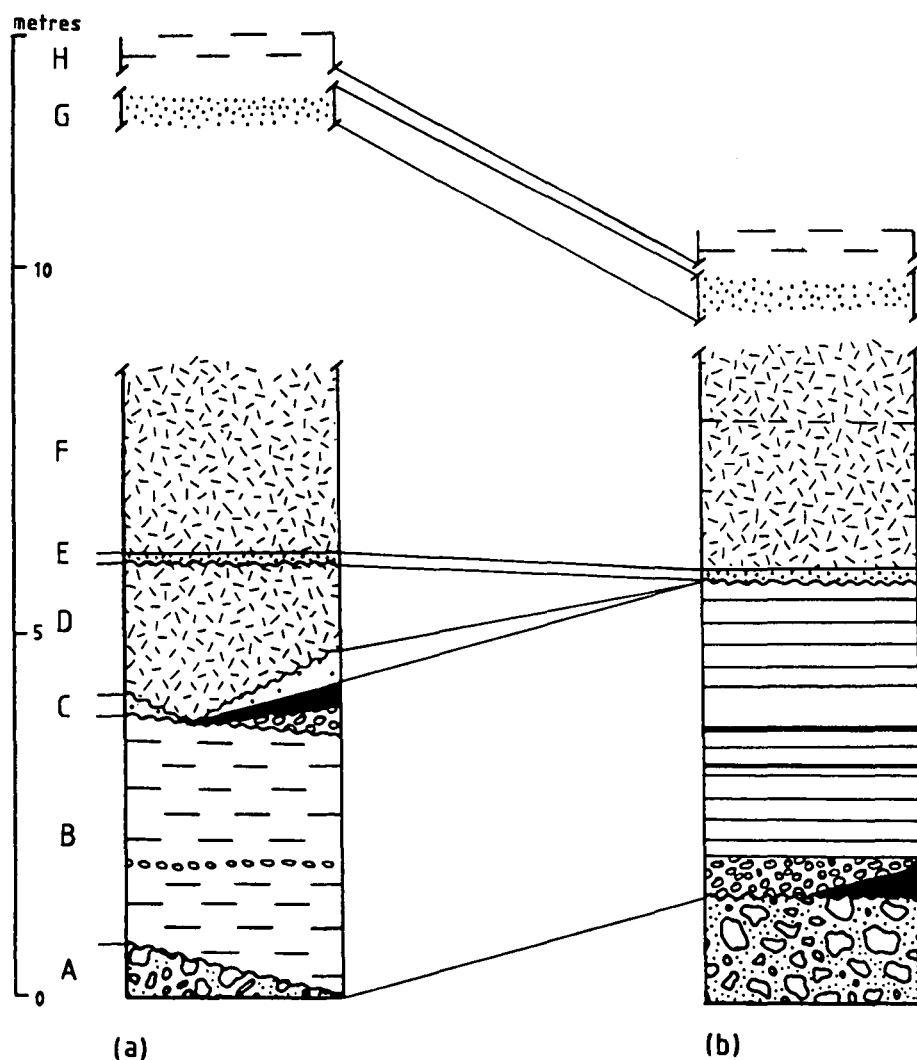Notice ultramafic xenolith with basalt crust (marked with arrow).

Fig. 11.
Location and definition of units in (a) cross-section II, (b) cross-section I.
A = pyroclastic flow deposit; B = epiclastic deposits; C = air fall deposit; D = reworked deposit I; E = pyroclastic surge deposit I; F = reworked deposits II; G = pyroclastic surge deposit II; H = lake deposit.
For legend see also Fig. 2.

The deposit is characterized by subangular to sub-rounded clasts in an open framework, by extremely poor sorting as well as by the absence of grading, bedding and other fabric features.

Of special interest is a degassing pipe which penetrates the pyroclastic flow deposit nearby cross-section I (Fig. 10). Degassing structures, enriched in coarse lithics and depleted in fines, are due to fluidisation in pyroclastic flows (CAS & WRIGHT, 1988), and indicate the hot emplacement of the deposit.

The heavy mineral spectrum of this unit shows a remarkable dominance of olivine (>70 grain %), followed by pyroxene, while the proportions of zircon, rutile, spinel, anatase, garnet and even hornblende are insignificant. However, olivine grains in the thin sections are not as common. This discrepancy seems curious, although it may be explained by the presence of olivine-rich ultramafic nodules (see section 2.2.).

### 3.2. Epiclastic and Reworked Deposits (Units B, D and F)

The sedimentary succession overlying the pyroclastic flow deposit consists of several beds of epiclastic and reworked material. They are exposed in the cliffs of the abandoned quarry near Beistein. Cross-section I (Fig. 4 and 11) shows the vertical sequence, which has been sampled according to obvious contacts, major uncon-

formities and characteristic changes within thicker beds.

Coarse, loose gravel containing epiclastic fragments, basaltic clasts and high amounts of quartz pebbles, overlies the tuff with a minimal dip towards southwest. The deposit forms a thin, discontinuous bed, though it may develop considerable thickness where it fills erosional channels. Local fine sediments show small crystallized wood remnants (<3 mm), vesicles and high white mica contents. Very well preserved fossil wood can also be found in a lenticular sandy bed at the same stratigraphic level.

The stratigraphically overlying beds A12, A11, A10, A9, A8, A7 and A6 are only slightly consolidated and show massive or planar bedding. Cross-bedding and grading (Fig. 12) are rare, although the variation of the grain size distribution is considerable (Tab. 4). Several sandy beds are interleaved with two thin fine-grained units (A8, A10). A few millimeters of muddy crusts at the base of A10 and A9 display shallow ripple structures which indicate a flow direction from northwest to southeast. Thin layers of coarser components (mainly mud balls and rounded epiclastic fragments of pyroclastic rock) mark the contacts A11/A12, A9/A10 and form a distinct horizon within A7.

The sandy and gravely beds A6, A7, A9, A11 and A12 show a predominantly closed framework. The ratio of basaltic to lithic components (approximately 1 : 1) stays constant, and the clasts are subangular to sub-
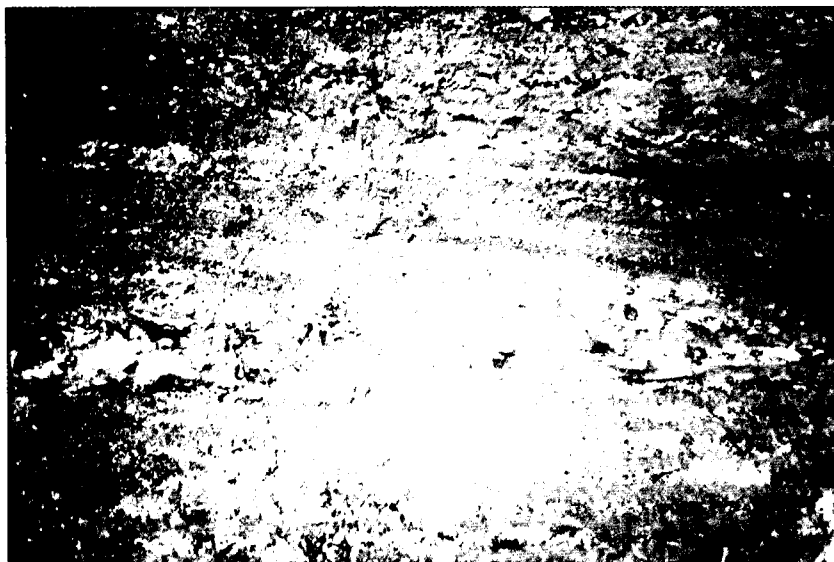
Fig. 12.
Epiclastic and reworked material (unit B) overlying pyroclastic flow deposit (unit A).

rounded. Olivine grains are common and the existence of rounded tuff fragments in each of the deposits mentioned above (including A5) proves their epiclastic origin.

Using a textural terminology for gravel-bearing detrital sediments (FAOLK, 1980) these deposits can be termed sands and sandy gravels (Tab. 4).

The median diameter (INMAN, 1952) ranges from $-0.35\Phi$ in gravel, to $3.9\Phi$ in muddy sand, and shows a random distribution through the vertical sequence, as does the INMAN parameter for sorting (Tab. 5). Considering the influence of hydraulic particle sorting (CAS & WRIGHT, 1988), which is enhanced by the broad range of density in volcaniclastic material, the deposits may be described as moderately to well sorted, although the values for sigma($\Phi$) are relatively high (0.7 to 1.95; Tab. 5).

The stratigraphically highest bed of the lower sedimentary unit, A5, shows quite different features, though the transition from A6H upwards to A5 is gradual. The material is consolidated enough to make a sieving analysis impossible but may—with the help of visual comparison diagrams—be termed poorly to moderately sorted, sandy gravel. Poorly rounded components form a closed framework lacking obvious structural features. The absence of abundant fine matrix gives rise to irregular vesicles of significant size. The

main components are lithic clasts (quartz, feldspars) and basaltic fragments.

The heavy mineral spectrum indicates a distinct dominance of olivine, followed by basaltic hornblende and clinopyroxene. Garnet is common. Orthopyroxene, spinel, rutile and zircon may occur, but do not exceed 2 grain percent each (Tab. 1 and 2.).

Several units of the sequence described in cross-section II exhibit different features. A partially exposed set of beds overlies the pyroclastic flow deposit. The volcaniclastic material with high proportions of clastic lithics and white mica crystals is thought to represent sediments deposited in a pond or lake. The overlying remnants of an air fall deposit with bomb sag structures, accretionary lapilli and normal grading is obscured by numerous minor unconformities. A lahar or debris flow deposit, that follows upwardly, unconformably filled an erosionally formed trough, and the bed is inclined towards the west (Fig. 2). Due to poor exposure, the lateral relationship of these units, along with their stratigraphic equivalents in cross-section I, is not thoroughly understood.

The three meter thick upper volcaniclastic unit in cross-section I overlies a prominent unconformity, (Fig. 2, 4 and 11) which is outlined by a thin layer of the pyroclastic surge deposit A4 (see section 3.3.). Different textural features, a sudden change from horizon-

| sample Nr. | gravel > 2 mm | sand 2 -0.063 mm | mud < 0.063 mm | class |
|---|---|---|---|---|
| * | wt.% | wt.% | wt.% | * |
| A2 | 4.8 | 91.1 | 4.1 | (g)S |
| A4 | 13.2 | 44.1 | 42.3 | gM |
| A6H | 0.3 | 97.1 | 2.2 | S |
| A6L | 0.0 | 98.9 | 1.1 | S |
| A7 | 33.8 | 62.9 | 3.3 | sG |
| A8 | 0.0 | 64.3 | 35.7 | mS |
| A9H | 9.7 | 81.1 | 9.2 | gmS |
| A9L | 17.9 | 78.7 | 3.4 | gS |
| A10 | 3.6 | 86.7 | 9.7 | (g)S |
| A11 | 34.9 | 62.0 | 3.1 | sG |
| A12/4 | 1.6 | 91.1 | 7.3 | (g)mS |
| A12/3 | 22.2 | 76.2 | 1.2 | gS |
| A12/2 | 20.4 | 77.3 | 2.3 | gS |
| A12/1 | 10.6 | 87.2 | 2.2 | gS |
| A13 | 0.0 | 54.9 | 45.1 | mS |

Table 4.
Classification of unconsolidated epiclastic sediments with respect to a textural terminology for detrital sediments (after FOLK, 1980).
sG = sandy gravel; gS = gravelly sand; gS = gravelly sand; gmS = gravelly muddy sand; gM = gravelly mud; (g)S = slightly gravelly sand; (g)mS = slightly gravelly muddy sand; S = sand; mS = muddy sand.

| sample | Md(phi) | Sigma(phi) |
|--------|---------|------------|
| A2 | 0.3 | 0.9 |
| A4 | 3.4 | 3.1 |
| A6H | 1.4 | 1.8 |
| A6L | 1.7 | 0.7 |
| A7 | -0.1 | 1.9 |
| A8 | 3.7 | 1.0 |
| A9H | 2.4 | 2.0 |
| A9L | 0.8 | 1.9 |
| A10 | 2.5 | 1.1 |
| A11 | -0.4 | 1.6 |
| A12/4 | 2.0 | 1.0 |
| A12/3 | 0.3 | 1.5 |
| A12/2 | 1.0 | 1.8 |
| A12/1 | 1.7 | 1.5 |
| A13 | 3.9 | 0.9 |

Table 5.
Grainsize parameters of median diameter and sorting for unconsolidated epiclastic sediments, derived graphically from cumulative curves.

tal bedding to an inclination of 35° and a distinct pyroxene peak in the heavy mineral spectrum indicate a sudden change of the depositional conditions (see section 3.3.).

Differences in grain size and color mark the contact between A4 and A3. The basal part of A3 contains lumps of fine light colored material of the underlying bed which must have been incorporated during the rapid deposition of the upper unit (see section 4.5.). Lithic and cryptocrystalline basaltic clasts (subangular to rounded) and a fine grayish matrix are densely packed in the open framework of the basal layers (A3). The sequence changes gradually upwardly, showing closed framework and high vesicularity. The matrix only encrusts the subrounded lithic and volcanic clasts, and diffuse stratification may interrupt the massive and disorganized texture (A2).

The coarse basal layer of the uppermost bed (A1) is steeply inclined (50° degrees) towards south-southwest. Subangular to rounded components (lithic and basaltic clasts) are imbedded in a cryptocrystalline matrix in an open framework. Vesicles are less common than in A2, although they are present.

Due to the high degree of consolidation, a sieving analysis was not possible. Based on visual estimation using comparison diagrams, the deposit may be described as poorly sorted. Clasts can be larger than 10 cm in diameter, but the average size is much below that.

The heavy mineral spectrum shows a drastic decrease of olivine in A1. Hornblende proportions often exceed 20 grain percent for this sequence; the contents of pyroxene, garnet and others (zircon, rutile, zoisit) vary.

A stratigraphically equivalent unit in cross-section II (Fig. 4 and 11) is thicker and shows some different features. Horizontal bedding seems to be absent, and the deposit is massive and strongly consolidated. Lithic and volcanic clasts (sub-angular) and a yellowish matrix are organized in an open framework. Clasts may be 10 cm in diameter and more.

Randomly distributed areas that are depleted in fines, or conversely, in coarse lithics, are characteristic for this sequence (A20, A21, A22, A23). They resemble irregular veins or diffuse streaks, and neither their spatial relationship nor their origin is understood.

The heavy mineral spectrum correlates positively with its lateral equivalent in cross-section I showing hornblende proportions that exceed 20 grain percent (Tab. 1 and 2.).

## 3.3. Pyroclastic Surge Deposits I, II (Units E and G)

### 3.3.1. Unit E

A steeply inclined layer of a yellowish fine-grained surge deposit (A4) marks a distinct discontinuity. The



Fig. 13.
Pyroclastic surge deposit I (unit E), unconformably overlying the epiclastic and reworked material (unit B).

deposit shows a thickness of 2–5 cm that may increase in depositional lows. It disconformably overlies the epiclastic and reworked material (Fig. 11 and 13) and is conformably overlain by a reworked (lahar) deposit A3 (see section 3.2.). The densely packed and consolidated material of this surge deposit contains abundant angular lithic clasts (quartz, feldspars), subspherical juvenile basaltic components and matrix, all organized in an open framework. Juvenile clasts generally have a crypocrystalline ground mass, but may also consist of brownish basaltic glass. The similarity of the phenocrysts (pyroxene, olivine) and the fact, that some single clasts contain glassy and cryptocrystalline groundmass, suggest an origin from the same magma batch (see section 2.3.2.). The microcrystalline matrix is slightly devitrified, though its glassy texture is locally preserved.

Pyroxene, amounting to 40 grain percent of the heavy mineral fraction (median out of 6 samples), is one of the dominant heavy mineral phases. The proportion of olivine (44 grain %) is low compared to values of the stratigraphically lower units, while amounts of hornblende (9 grain %) are not exceptional. The presence of garnet, with 6.1 grain percent, may indicate that the vent-forming explosion cut into a sedimentary layer rich in garnet. Proportions of rutile, zircon and spinel are insignificant (Tab. 1 and 2).

### 3.3.2. Unit G

This sequence of pyroclastic surge deposits is the only unit that can be traced laterally over longer distances. It is exposed at the top of the quarry cliffs, and along the flanks of the hill. The succession represents the ancient crater rim and the individual beds are steeply inclined towards the center of this crater (see section 1.4. and Fig. 5). The contact with lower sequences is not exposed.

Six samples have been taken: S10 to the south of the quarry cliffs, S9 and S8 nearby the two cross-sections, S7, S6 and S5 along the lateral extension of the unit, where the strike gradually turns from an east-west direction to north-south (Fig. 5).

The deposits show distinct syn-depositional structures. Low-angle-cross-stratification is well developed

in S6, S8, S9 and S10 (Fig. 14). Few impact structures are exposed, where the ballistic ejecta are generally weathered out. The grainsize varies widely between individual layers. Thin fine-grained (ash) beds are as common as beds containing coarse lapilli, indicating varying strenght of the eruption pulses that gave rise to the deposits. Although sorting is generally poor, some coarse layers may be strongly depleted in fines (S10). Closed framework and numerous irregular air spaces are occasionally observed in lapilli-dominated beds (S10), while layers with an abundant ash-size fraction show a densely packed organization of clasts and matrix in an open framework.

Dense basaltic components are generally larger and better rounded (subrounded) than the lithics. Lithics are of angular to subangular pieces of broken quartz pebbles, feldspars, metamorphic and clastic lithic rocks. The ratio of basaltic versus lithic clasts may differ between individual layers, though commonly basaltic clasts are dominant in coarse and fines-depleted lapilli beds. Of special interest is the occurrence of accretionary and armored lapilli, which are accretions of ash-size particles around a water droplet or a solid particle (S6, S8, S9, S10). They indicate a wet depositional environment. Due to alteration processes, such as devitrification, the small, rounded aggregates may appear diffuse but are readily distinguishable in thin sections (Fig. 8).

The originally glassy ash matrix has undergone extensive alteration in most deposits and shows a cryptocrystalline texture. The alteration processes, however, have not affected the thin, densely packed fine-grained layers in unit S10, where the remnants of matrix is isotropic and seems to represent the original vitric ash shards.

For samples S5, S6, S8, S9, and S10, the heavy mineral analysis shows a consistent pattern (Tab. 1 and 2): Pyroxene (33.3–56.5 grain %) dominates over olivine (18.8–38.5 grain %) and hornblende (15.0–32.3 grain %). Garnet, spinel and rutile occur in insignificant amounts. Sample A7, containing 59.6 grain percent olivine, 21.0 grain percent hornblende and minor amounts of other minerals, does not correlate with that pattern, and the absence of accretionary and armored lapilli may indicate a genetically different origin (see section 5.3.).
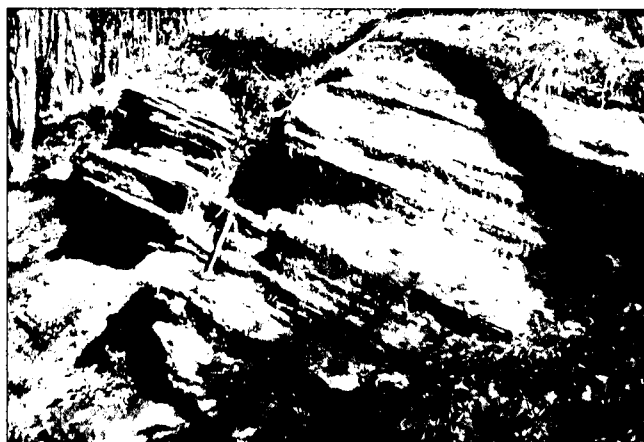


Fig. 14.
a) Low-angle-cross-stratification in pyroclastic surge deposit II (unit G).
b) Close-up.

## 3.4. Air Fall Deposit (Unit C)

Samples A30 and A31 (cross-section II; Fig. 4) are thought to represent the remnants of an air fall deposit. Normal grading of the predominantly sand-sized components is a characteristic that distinguishes this unit clearly from the remaining deposits. Basaltic bombs and impact structures mark a distinct horizon within the deposit. Accretionary and armored lapilli indicate a wet depositional environment.

## 3.5. Lake Deposit (Unit H)

A sequence of thin beds forms the uppermost unit of the volcaniclastic succession. The material is slightly consolidated. Fine-grained layers of clay minerals are interleaved by coarser beds containing basaltic clasts. The occurrence of basaltic bombs and impact structures within the coarser layers indicate their pyroclastic origin (Fig. 15 (a)). A paleo-mud-boil, that penetrates the sequence (Fig. 15 (b)), and the generally strong alteration of the basaltic material results from hydrothermal activity during and after the time of deposition.

# 4. Sequence of Events and Discussion of Depositional and Physical Processes

The following discussion is based on observations made and data derived from the very confined area as described above. Eventual conclusions are not necessarily valid for all nearby basaltic volcaniclastic deposits, and this constraint should be kept in mind. However, the physical and depositional processes involved are anticipated to remain within a small range of variations, if one considers the general similarities of the country rock, ancient environments and features of the deposits. Consequently, the presented model may very well be representative for the main mechanisms that led to the deposition of volcaniclastic deposits throughout this area.

The succession exposed at the quarry cliffs and described in two cross-sections and several nearby outcrops indicate hydrovolcanic activity, that produced a variety of volcaniclastic material. Hydroclastic eruptions result from the interaction of magma and external water. Water sources may be superficial (lake, sea, river) or groundwater reservoirs. The sediments of the Tertiary Basin, however, have high groundwater capacities (EBNER et al., 1985), and several aquifers may have provided abundant water for an explosive interaction with magma. The ascending magma directly contacted groundwater, and the resulting eruption produced juvenile, cognate and accidental ejecta (CAS & WRIGHT, 1988; FISHER & SCHMINCKE, 1984). According to the international nomenclature, eruption styles showing these features are also termed phreatomagmatic. In regard to the geometry of the deposits, the quarry cliff is thought to expose one section of the inner crater. The geometry of the individual deposits and their spatial relationships with each other subdivide the sequence into the previously described units (Fig. 11), which are discussed in the following sections according to the sequence of volcanic events (Tab. 6).

## 4.1. Pyroclastic Flow Deposit (Unit A)

The pyroclastic flow deposit (unit A) and the overlying volcaniclastic sediments (B, C, D; compare Fig. 2, 4 and 11) are thought to represent material from a provenance, which is not included in this study. Regarding the low relief of volcanoes in basaltic volcanic fields, the generally limited volume of pyroclastic flows in such an environment and the relative thickness of the present pyroclastic flow deposit, the source of the material is thought to be located nearby. If the fine-grained layered sediments at Burgfeld, a few kilometers to the northwest of Beistein, represent the late lake deposit of a maar crater, the origin of the sequence studied may be explained by earlier volcanic activity and subsequent erosional processes at this nearby eruptive center. The low inclination of the beds towards the southeast is due to the low topographic slopes typical for maars and tuff rings.

Based on its descriptive features such as abundance of matrix, non-vesicular to slightly inflated juvenile fragments, extremely poor sorting and lack of fabric structures, the basal unit may be classified as a block-
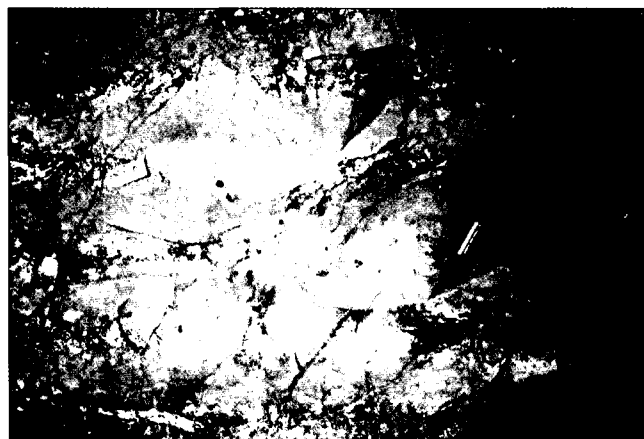


Fig. 15.
Lake deposit (unit H).
a) Bomb sag structure.
b) Paleo-mud-boil penetrating the deposit.

| regional processes | local processes | resulting deposits |
|---|---|---|
| end of lacustrian-fluvial sedimentation, high topographic relief | | |
| Pliocene volcanism in baslatic volcano field | deposition of pyroclastic flow deposit derived from eruptive center to the NW | pyroclastic flow deposit |
| | deposition of volcaniclastic and clastic material, presumably derived from slopes of an eruptive center to the NW and nearby non-volcanic areas | epiclastic deposits (unit B) |
| | ash-fall due to volcanic activities nearby | air fall deposit (unit C) |
| | erosional processes in alluvial fan environment | local debris flow deposits (unit D) |
| | hydrovolcanic eruption due to interaction of magma and ground water | surge deposit (unit E) |
| | erosional processes in vent area (collapse of crater walls, lahars, etc.) | lahar deposits (unit F) |
| | hydrovolcanic eruption due to interaction of magma and ground water and/or crater lake water | surge deposits (unit G) |
| | end of volcanic activity, sedimentation of crater lake deposits, continuing heat flow and hydrothermal activity | lake deposit (unit H) |
| | erosional processes removing most of the edifice | |

Table 6.
Schematic diagram: Sequence of events.
For further explanation see text (chapter 4.) and Fig. 16.

and ash-flow deposit (CAS & WRIGHT, 1988; FISHER & SCHMINCKE, 1984). The abundance of accidental clasts indicates the hydroclastic mechanisms that are characteristic for shallow phreatomagmatic eruptions.

CAS & WRIGHT (1988) mention the similarity of lahar deposits to nonwelded pyroclastic flow deposits. One major distinguishing criteria suggested by them is the occurrence of degassing features, which prove the hot emplacement of a pyroclastic flow, although gas-escape tubes have been described in hot lahar deposits also (ARGUDEN & RODOLFO, 1990). The degassing pipe, exposed near cross-section I in unit A, penetrated the deposit and propagated through to the bed surface during formation. Gas segregation structures are generally not longer than approximately 50 cm (CAS & WRIGHT, 1988). The structure at issue is seen over a length of 2 m, and may continue downwards where the deposit is not exposed. Its dimension suggests either an extensive external water source, that provided enough steam to elutriate the material thoroughly, or a long-lived internal gas source such as a fumarole. The absence of oxidation and alteration of the adjacent material, which commonly accompany fumarolic activity, favors the idea of steam derived from external water.

Poor sorting and the lack of fabric structures are usually attributed to high particle concentration rather than turbulence (CAS & WRIGHT, 1988). Intact, but slightly deformed and marginally altered mud lumps within the deposit may provide further evidence for laminar flow conditions in the body of the pyroclastic flow. This corresponds with the conclusions of several studies on this subject (SPARKS, 1976; SPARKS et al., 1978; SHERIDAN, 1979). Because fragile clasts such as aggregates of coarse olivine grains are most likely to break during secondary depositional processes, the presence of large ultramafic nodules in unit A might be another indicator for its pyroclastic origin.

The occurrence of ultramafic nodules (Fig. 9) in the deposit is not restricted to this specific unit, but is typical for many volcaniclastic deposits of the volcanic field. Xenoliths of the composition found in this unit (see section 1.3.), are apparently of mantle origin and characteristic for alkali- and nepheline-basalts, particularly the very silica-poor varieties. HESS (1989) points out that magmas, capable of carrying large mantle fragments to the earth's surface, must have been derived directly from the mantle without undergoing near-surface crystal fractionation. Nodules of the size found in this unit also seem to imply a fast ascent of the low-viscosity basaltic melt, fast enough to prevent gravitational removal of the heavy clasts. At subliquidus temperatures though, the presence of rigid crystals impedes the flow of the magma, and therefore, may increase the apparent viscosity significantly. The crystal-liquid-suspension loses the viscometric properties of a Newtonian liquid. According to calculations, the corresponding yield strengths in partially crystallized basalts may be large enough that big xenoliths remain suspended in the magma. Experiments have shown that the apparent viscosity of a suspension decreases once flow is initiated (HESS, 1989). In regard to additional information, such as the absence of alteration affecting the various xenolithes, it may be safely as-

sumed that the melt ascended with considerable speed and that a possible increase of viscosity was not significant.

## 4.2. Epiclastic deposits
## (Unit B)

The close relationship between sedimentary and pyroclastic deposits in volcaniclastic environments is an essential factor in facies modelling. Sedimentary successions characterize long-lived periods of volcanic quiescence, which are dominated by epiclastic processes. The lack of vegetation, a high relief, and the abundance of loose debris, enhance the influence of physical processes such as gravitational collapse and running water (rivers, rain water, melt water), which accelerate the erosion rate (FRANCIS, 1983; CAS & WRIGHT, 1988).

Erosion, transport and sedimentation of volcanic rock or tuff produce epiclastic fragments, which form new sedimentary deposits. Reworking and remobilization of loose, unconsolidated pyroclastic debris give rise to deposits that can barely be distinguished from the original deposit, if at all (FISHER & SCHMINCKE, 1984).

VESSELL & DAVIES (1981) documented the close temporal relationship between volcanic and epiclastic processes in the Guatemalan chain. They mention the characteristic fan-building phase following an eruptive phase and divide nonmarine volcanic deposits from active, flow producing volcanoes into the following four facies:

1) The vent facies consists of interbedded lavas, fallout tephra and breccias caused by erosion on steep flanks.
2) Proximal and
3) medial facies (near-source-facies, FISHER & SCHMINCKE, 1984) show pyroclastic flow breccias, eroded debris and fallout tephra as valley fills, grading into alluvial fans (debris flows, tephra and fluvial debris) at the base of the volcano.
4) The distal facies (intermediate-source-facies, FISHER & SCHMINCKE, 1984) consists of fluvial deposits interbedded with tephra layers.

Similar conditions may have been of importance in the depositional history of the Beistein succession, and according to the descriptive features of the deposits (see section 3.2.), the lower sedimentary unit in cross-section I is thought to represent alluvial fan deposits.

The coarse gravel filling erosional channels and the sandy layers, that show parallel bedding and rare planar cross-bedding, are characteristic for mid-fan areas. Sandy and silty sediments with parallel bedding, low-angle planar cross-bedding and rare ripple-bedding are common in sheet flood deposits of the distal facies (REINECK & SINGH, 1980). The flow direction shown by ripple structures within these layers (see section 3.2.) indicates, that the material has been derived from the eruption center at Burgfeld and deposited on top of the previously emplaced pyroclastic flow deposit (see Fig. 16). Thin layers of gravel and the occurrence of armored mud balls, such as seen within the sediments (see section 3.2.), have also been described in non-volcanic alluvial fan deposits. Volcaniclastic deposits are frequently poorly sorted and may show modified textures according to the variation in density of their

clasts (see section 3.2.). Therefore, the epiclastic succession as described in section 3.2. (A13–A5) may represent deposits emplaced in an alluvial fan environment. Generally, low slopes of the proposed maar environment will modify the depositional conditions, and hence can explain the dominance of mid-fan and distal fan facies. Of course, the prevailing facies association may simply reflect the topographic position of the outcrop with respect to the source.

Based on studies of the specific processes, SMITH (1986) proposed the term "hyperconcentrated flood flow" for describing depositional conditions intermediate between debris flow and stream flow. Clast support, horizontal stratification, lack of cross-stratification in sandy deposits and poor sorting, which are features characteristic for hyperconcentrated flood flow deposits, are due to high discharge rates common on arid alluvial fans. Because of much larger volumes of easily eroded pyroclastic debris and unvegetated slopes in volcanic regions, these deposits are not only most common, but have greater preservation potential, show greater lateral variability and are more voluminous (SMITH, 1986). Characteristic lack of cross-stratification and poor sorting in the sequence at issue may indicate that hyperconcentrated flood flows were a significant factor in the emplacement of the deposit. The question remains whether or not high rates of precipitation, a general climatic characteristic of periods preceding ice-ages, and the abundance of loose debris are enough to compensate for the lack of high slopes.

The epiclastic lake sediments overlying the pyroclastic flow deposit in cross-section II must have been deposited within the same time interval as unit B (A5 to A13) in cross-section I. Abrupt changes of depositional conditions within such close spatial spacing may occur in volcanic environments but, the exact lateral relationship is not understood.

The abundance of lithic components in the channel-filling, coarse gravel in cross-section I, and in several other layers, is not sufficiently explained by sorting phenomena of lithic-rich volcaniclastics. One plausible explanation is for a nearby non-volcanic hinterland to provide clastic material to the transition zone of the distal fan. In this case, the surrounding Tertiary sediments must have had a considerable relief at the time of volcanic activity. This is also indicated by the occurrence of post-basaltic pebbles at relatively high elevations (see section 1.3. and Fig. 3).

## 4.3. Air Fall Deposit
## and Reworked Deposit I
## (Units C and D)

The only air fall deposit seen in the outcrop is a remnant (unit C, see Fig. 2 and Fig. 11). Erosionally truncated and obscured by numerous small discontinuities, it appears to lie stratigraphically below surge deposit I, unit E, and above the pyroclastic flow deposit, unit A. Therefore, it must be derived from another eruptive center. Bomb sag structures of significant size indicate that the source for this deposit was nearby and/or that the energy of the eruption must have been considerable. Accretionary and armored lapilli within the normally graded deposit show that steam explosions were also characteristic for adjacent eruption centers. A very fine-grained air fall deposit near Zinsberg contains big
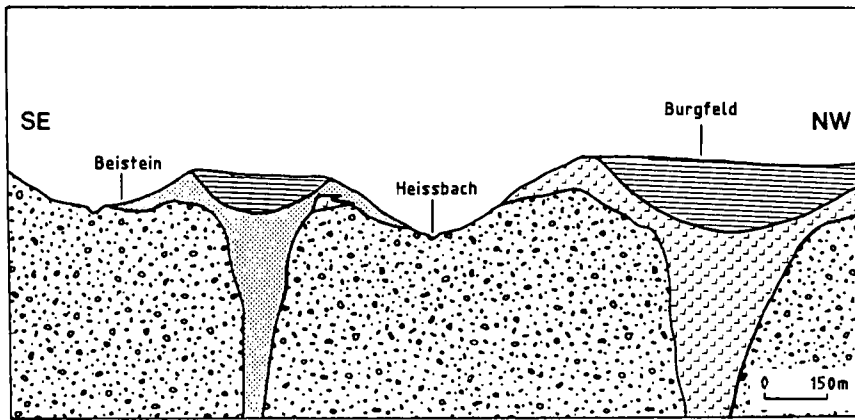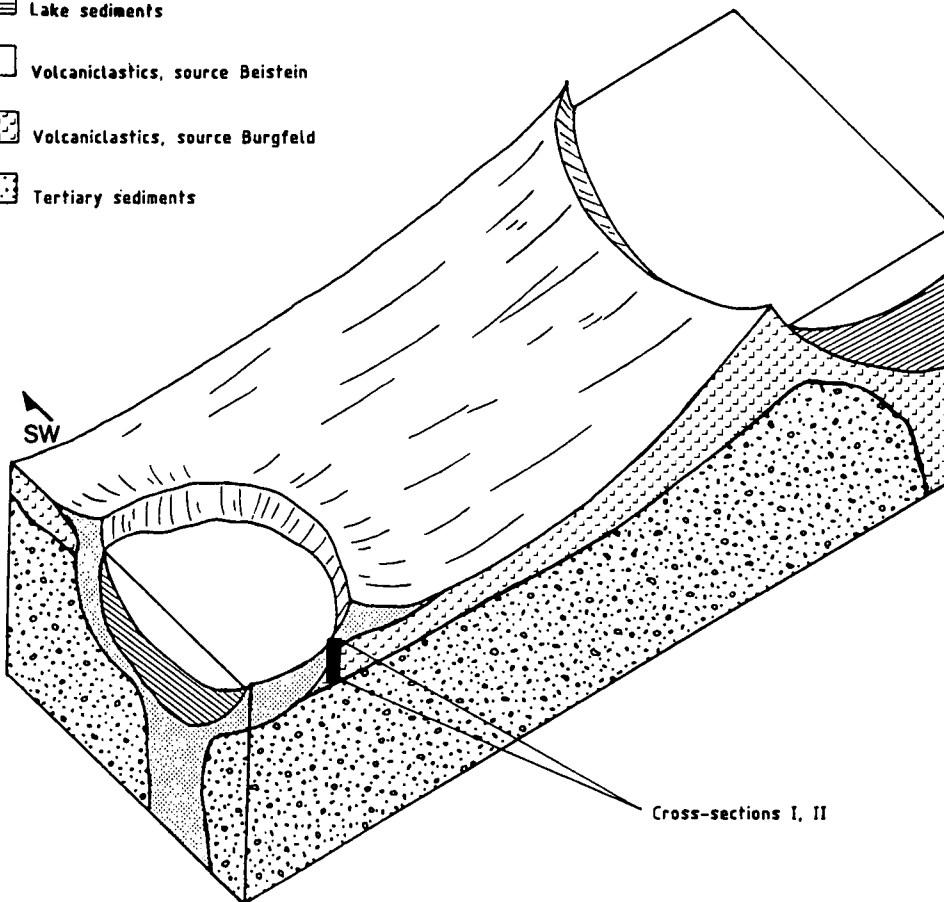
Fig. 16.
Schematic model for the volcani-
clastic succession near Beistein.
a) Generalized cross-section sho-
wing present relief.
b) Reconstruction of the assumed
maar-environment at the time of
volcanic activity.

accretionary lapilli, but its spatial relationship with re-
spect to the Beistein sequence is not understood.

The overlying lahar deposit (unit D; Fig. 11) seen in
cross-section II is also restricted in extension and vol-
ume. Small-scale erosional processes in the alluvial fan
environment may have led to local deposition in chan-
nels.

### 4.4. Pyroclastic Surge Deposit I
(Unit E)

Outlining a main unconformity (Fig. 2), unit E (layer
A4; Fig. 11) provides evidence for a dramatic change of
the depositional conditions. The steep inclination indi-
cates a powerful volcanic eruption that cut into the
nearly flat succession in cross-section I, and may have

approximately followed and steepened the pre-existing
slope shown in cross-section II. A thin pyroclastic
surge deposit (see section 3.3.1.) seems to be plas-
tered against the slope. Similar deposition of pyroclas-
tic surges has been reported from historic maar-erup-
tions (KIENLE et al., 1980); evidence for energetic
surges that travel up steep crater walls has also been
found in ancient maar deposits (WOHLETZ & SHERIDAN,
1983).

The occurrence of sideromelane shards, glassy ma-
trix, slightly vesicular subspherical lapilli, and abundant
accidental lithic clasts, is another major argument for a
steam explosion, which is the main eruption
mechanism leading to the formation of maar and tuff
rings. The low vesicularity of the densely packed, con-
solidated tuff suggests hot emplacement by a dry base
surge. Dry surges are deposited above condensation

temperature, and the super-heated steam is mostly lost prior to emplacement. Consequently, trapping of water droplets and the eventual formation of vesiculated tuff with high porosity is unlikely.

SHERIDAN & WOHLETZ (1981) point out that eruptions leading to dry base surges imply moderate water/ magma ratios (0.3 to 1.0), where superheating, energy transfer efficiency, magma fragmentation and eruptive energy are extremely high. Small clasts and the high proportion of ash-sized matrix of the deposit in question indicate a high degree of fragmentation. Superheating and efficient heat transfer leading to rapid cooling may have caused the formation of chilled sideromelane shards.

Several aquifers within the Tertiary successions may have provided abundant groundwater for an explosive interaction with ascending magma, which in turn gave rise to the crater deeply cut into the country rock. The lithic clasts, predominantly quartz grains and fragments of broken quartz pebbles, represent material from the underlying sediments. These have been penetrated by the ascending magma and ejected during the shallow explosions of the crater-forming phase (LORENZ, 1973, 1986). Quartz grains can even be seen within basaltic lapilli. The nephelinitic and olivine-basanitic composition of the magma (see section 1.2.) excludes the presence of modal quartz in the basalt, and the grains have been incorporated as xenoliths on the way upwards. The usual lack of reaction rims and alterations on quartz grains gives evidence for the fast ascent of the magma, leaving no time for the re-establishment of equilibrium conditions.

Typical maar-forming eruptions produce explosion breccias that are coarse-grained and chaotic, and contain a variety of angular fragments of broken countryrock (WOHLETZ & SHERIDAN, 1983; CAS & WRIGHT, 1988). These features are observed in the underlying bed A5, which is – in contrast to the remaining layers of unit B – strongly consolidated. The absence of an expected discontinuity and the gradual transition between A6H and A5, however, make an explosive origin of this deposit doubtful. Furthermore, unconsolidated surficial material may cause the absence or poor development of explosive breccias, as WOHLETZ & SHERIDAN (1983) pointed out in their general study "Hydrovolcanic Explosions II". The high degree of consolidation may be due to high temperatures during the deposition of the overlying pyroclastic surge deposit.

Increased proportions of pyroxene in the heavy mineral spectrum confirm the hypothesis of an initial vent-forming explosive event. The renewed volcanic activity and the slightly modified mineralogical assemblage in the involved magma may be consequences of melting processes or changing conditions in the magma reservoir.

## 4.5. Reworked Deposits II (Unit F)

The event documented by the pyroclastic surge deposit (A4) and the underlying steeply inclined discontinuity changed the depositional conditions. The steep slopes of the inner crater walls enhance processes such as grain flow, particle creep and lahars associated with hyperconcentrated streamflows (CAS & WRIGHT, 1988; ARGUDEN & RODOLFO, 1990).

Grain flow and particle creep occur where cohesionless grains have enough gravitational potential to move downslope spontaneously, although on exposed slopes, rainfall, surface water, sheet flow and wind are at least periodic causes of movement. Initiated by oversteepening, common on steep inner crater walls, scree slopes will form and provide the physical conditions for the processes as mentioned above. The deposits are marked by steeply inclined and internally diffuse stratification (CAS & WRIGHT, 1988) such as that seen in layer A2. Gravitational collapse of crater walls and the subsequent development of scree slopes have been observed during and after several historic maar-eruptions (KIENLE et al., 1980; SELF et al., 1980; LORENZ, 1973, 1986).

Lahars or volcanic debris flows are commonly associated with stratovolcanoes and may deposit significant volumes of volcanic debris. Lahars of much smaller dimensions have been reported from phreatomagmatic eruptions (FISHER & SCHMINCKE, 1984). They are thought to result from collapse of crater walls or instability of water saturated debris on steep slopes and frequently accompany eruptions (FISHER & SCHMINCKE, 1984; CAS & WRIGHT, 1988). Water is a major lubricant in these flows, though the transport medium is cohesive mud, a non-Newtonian fluid with a yield strength. The high bulk density, and the therefore significant strength capable of supporting large clasts, influence the final depositional structures (CAS & WRIGHT, 1988). Lahars usually follow depressions, leaving thin deposits on steep slopes and thicker deposits on valley-bottoms. Commonly lahars overlie the depositional surface conformably, although, due to local turbulence or steepness of the slope, surface material may be incorporated (FISHER & SCHMINCKE, 1984). The occurrence of fine-grained, yellowish streaks (derived from A4) in the basal part of A3 and the steep inclination of this bed, strongly indicate that a lahar gave rise to this deposit. This conclusion is emphasized by its extremely poor sorting and characteristically subangular to subspherical clasts in an open framework, which correspond perfectly with the general features of lahar deposits (CAS & WRIGHT, 1988). Similar phenomena are found in A1 and many beds in cross-section II (A20, A21, A22, A23) which are thought to have the same origin. The thickness and the slightly different texture of the lahar deposit in cross-section II may reflect local differences of topographic position. Cross-section II seems to expose a local topographic low (channel, chute), cross-section I a topographic high, respectively. Unit F (Fig. 11) includes the deposits of both cross-sections that show those mutual features and have the same stratigraphical level.

Air spaces or vesicles in lahar deposits have been described and explained as trapped air bubbles by CRANDELL & WALDRON (1956) and CRANDELL (1971). The cavities seen in the lahar deposits at Beistein (A1, A3, A20, A21, A22, A23, A25, A27) are not spherical but irregular spaces where matrix is missing in between adjacent clasts. Hence, they are thought to have formed by draining away water after deposition.

CRANDELL (1971) points out a subtle grading of the coarse-grained dispersed phase, while ARGUDEN & RODOLFO (1990) state that inversely graded basal layers are common in hot lahar deposits but minor and neg-

828

lectable in cold ones. Of those deposits in question, only A1 shows a coarse basal layer which marks a contact. The randomly distributed streaks and veins (see section 3.2.) that are seen throughout the upper sequence of profile II show no specific pattern, and their origin is not understood.

## 4.6. Pyroclastic Surge Deposit II (Unit G)

The last volcanic event at this eruptive center is documented in the sequence of pyroclastic surge deposits (unit G, samples S5, S6, S8, S9, S10; Fig. 11) which describe the ancient crater rim (see Fig. 5). Sample S7 was originally thought to represent a pyroclastic surge deposit. Distinct differences of the heavy mineral spectrum and textural features as well as the lack of accretionary and armored lapilli make this assignment doubtful. The exact stratigraphic relation is not obvious, but the sample may belong to the underlying lahar deposits (unit F). This discrimination is confirmed by statistical analysis (see chapter 5.). The assumed thickness (>2 m) of the succession and the change of depositional structures indicate a multiphase eruption under varying conditions. In regard to the relatively consistent geochemical composition and the absence of paleo-soil, the succession is thought to be deposited within the course of one eruption.

Based on the spatial geometry of the bed, it is assumed that the eruption took place inside the pre-existing crater that was formed during the initial explosion. The surges moved uphill on the inner sides of the crater rim, which is thought to be a common mechanism in maar volcanism (FISHER & WATERS, 1970; KIENLE et al., 1980; WOHLETZ & SHERIDAN, 1983). Most deposits show a very low-angle-cross-stratification, which is due to high initial velocities and turbulence (CAS & WRIGHT, 1988). WOHLETZ & SHERIDAN (1974) state, that changing flow conditions, with respect to time and distance, cause a depositional sequence. The dominating low-angle-cross-stratificated and interbedded massive beds, exposed at Beistein, are characteristic for near-vent sandwave facies corresponding to their spatial position.

The numerous, thinly bedded deposits, exhibiting subtle differences in their depositional features, may reflect a varying influx of magma and water into the mixing space (SHERIDAN & WOHLETZ, 1981). This produces pulsating eruptions with oscillating explosive energy and, consequently, changing velocities of the resulting base surges. Oscillations in the intensity of explosions may also be caused by vaporization waves related to the explosive transition from superheated water into expanded vapor (BENNETT, 1972). Both mechanisms produce lateral blasts, which are due to the expansion of a superheated steam mixture that reaches low confining pressures at the surface (SHERIDAN & WOHLETZ, 1981). Lateral blasts are common in hydrovolcanic eruptions and may explain the dominance of surge deposits and the scarcity of air fall deposits in the sequence. Rare air fall deposits may have been of small volume to begin with, and later rapidly eroded.

A newly formed crater lake may have supplied abundant water for a hydrovolcanic eruption with high water/magma ratios (>1, SHERIDAN & WOHLETZ, 1981)

leading to a sequence of cool and wet surges. Magma fragmentation and eruptive energy on these conditions are relatively low explaining the coarser grain-sizes shown in unit G. Due to low superheating and heat transfer efficiency the ash is nearly saturated with water. Consequently trapped air or steam can not escape which, leads to moderate to high vesicularity, a characteristic feature of many layers of pyroclastic surge deposit I (unit G).

## 4.7. Maar Volcanism

Because of the numerous features indicating shallow phreatomagmatic explosions, lateral blasts are thought to be the main mechanisms for the emplacement of the pyroclastic surge deposits. In regard to the spatial distribution of exposed Tertiary sediments, the low rim formed by surge deposits describes a small crater, that was cut into the country rock below the general ground level (Fig. 16). The Tertiary sediments and the volcanicalstic deposits derived from the nearby eruption center at Burgfeld were penetrated by the initial explosion. Abundant accidental ejecta and the described geometry are characteristic for maar volcanoes. Maars occur frequently in monogenetic basaltic volcano fields. They are commonly formed in groups and related to underlying diatremes (LORENZ, 1973, 1986).

According to the depositional features of the surge deposits, the maar-forming eruption produced a hot, dry base surge that gave rise to the dense deposit A4. During a supposedly short time of quiescence, collapse of the inner crater walls, spalling and erosional processes formed a sequence of reworked material (A3 to A1, A23 to A20). Renewed influx of magma and larger volumes of external water triggered another eruption or eruption phase. Water was derived from an aquifer within the countryrock, or from a lake that may have formed in the crater. The source, however, must have provided abundant water to produce the thick sequence of predominantly wet surge deposits. Volcanic activity ceased soon afterwards, and the magma may have never reached the surface. Post-eruptive lake sediments (unit H; Fig. 11) were deposited in the crater. Volcaniclastic dominated layers and bomb sag structures (Fig. 15 (a)) give evidence for the proceeding volcanism nearby. A palaeo-mud-boil that penetrates the lake sediments (Fig. 15 (b)) indicates continuing high heat flow and hydrothermal activity (Tab. 6).

LORENZ (1973) points out that subsidence of the wallrocks, due to critical pressure differences and size and shape of the eruption chamber, may lead to the formation of ring-fault systems. It is possible that subsidence did take place at the Beistein crater, and that the resulting unconformities are simply not exposed or covered by younger material. The relative smallness of the crater and the restricted number of volcanic events documented in the sequence, indicate a short-lived volcanic activity at this particular eruption center. It may have, therefore, never reached the state of major subsidence.

## 5. Statistical Processing

### 5.1. Methods and Procedures

Data for multivariate analysis methods are taken from both, the heavy mineral and the component

analyses (see section 2.). Both data sets are closed systems in which the variables measured add to a fixed total of 100 %. This can, consequently, induce negative correlation effects on any possible result, which should be taken in consideration for interpretations. Factor Analysis (R-mode method) is designed to reveal underlying structures within a set of multivariate observations. Patterns and combinations of the factor loadings provide information about the correlation and the significance of single variables for the internal structure of the data set (see DAVIS, 1986). The structures revealed in this study seem to match the presumed patterns derived from geological field studies. Interrelationships of variables shown by factors, however, should be interpreted carefully and checked against the geological observations.

A reasonable distinction between stratigraphic units within the two cross-sections requires an essential assumption: The variance among the vertical samples must be significantly larger than the variance of lateral samples that are thought to belong to the same unit. This means that the variance among the vertical samples of each cross-section must exceed the variance between the two cross-sections. Multivariate Discriminant Analysis (MDA) provides a linear combination of selected variables, which produce the maximum difference between the previously defined groups (see DAVIS, 1986; BMDP (SOLO), 1989).

Assuming the classification of the units of cross-section I, based on geological features and stratigraphic relations, is valid, five groups are defined:

○ Pyroclastic flow deposit A (classification samples: A14B, A14C, A14D)
○ Reworked (epiclastic) deposit B (classification samples: A6H, A9H, A10, A12/3)
○ Surge deposit E (classification samples: A4A, A4B, A4C)
○ Reworked deposit F (classification samples: A1, A3)
○ Surge deposit G (classification samples: S8, S9, S10)

The remaining samples are assigned to one of the previously defined groups, which form the base set for the dependent variable in the analysis. In regard to the inconsistency of the beds throughout both cross-sections, the observations of units C and D were eliminated from the data set. Unit B was included only in Analysis 1. By defining groups for the dependant variable according to an unverified classification scheme, the resulting analysis may be incorrect. One simple way of testing the significance of the Multivariate Discriminant Analysis and the previous classification on which it is based on, can be achieved by classifying the groups with an independent Cluster Analysis. The resulting clusters can then be used for the dependent variable in another set of Multiple Discriminant Analyses. Comparisons between the results of the outputs allows for assessment of the significance of the previous classification. Comparisons may also reveal misclassifications and the effects of disturbing influence of trendless variables. This information can help with the interpretation of the data set and/or confirm
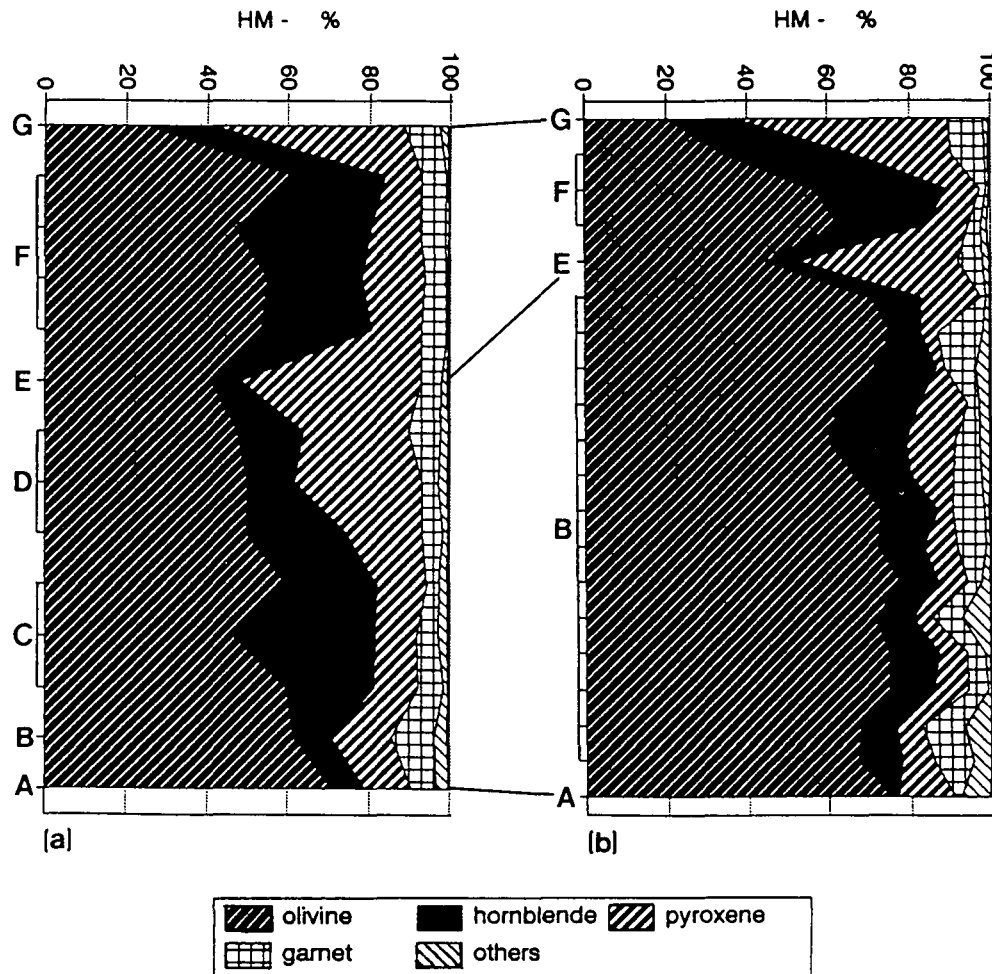


Fig. 17.
Distribution of heavy minerals in
a) cross-section II,
b) cross-section I.
Vertical scale does not correspond to distances within the profiles.
For definitions of units A to G see Fig. 11.

olivine    hornblende    pyroxene
garnet    others

the interpretation derived from geological considerations.

When modelling the complete heavy mineral data set, all samples are included. The data derived from the component analysis cover only the pyroclastic flow deposit (A), the reworked deposit (F) and the surge deposit (G). Therefore units B and E are ignored when only component data or the combined set of heavy mineral and component analyses are examined.

The step-wise Multivariate Discriminant Analysis program and the results of Factor Analysis, both backed up by geological observations, make it possible to distinguish those variables that have the most significant impact on the variance. In some cases the results of analyses could be considerably improved in accuracy if a carefully limited set of variables was used.

The interpretations derived by the numerous statistical methods should be accompanied by theoretical and logical considerations. Results are meant to confirm, specify or falsify the previously established model rather than to produce new ideas.

All analyses were run on programms of the SOLO statistics computer package (BMDP, Statistical Software Inc., 1988).

## 5.2. Underlying Structures in the Multivariate Data Set (Factor Analysis)

Based on field observations, an underlying structure within the data set is presumed to exist. The heavy mineral distribution shows distinct correlations between the two cross-sections (Fig. 17). Sharp peaks of minerals olivine and pyroxene mark the pyroclastic deposits. High amounts of olivine (exceeding 70 grain %) characterize unit A, the pyroclastic flow deposit. A sudden increase of pyroxene marks both surge deposits (units E and G). The differences of the heavy mineral spectra may indicate different sources.

Secondary erosional processes involve material with different origin. The heavy mineral data as well as other features (component analysis) are likely to loose their original characteristics due to mixing effects. Therefore

it is not surprising, that data of both epiclastic fluvial deposits (unit B and C) and reworked deposits (units D and F) are smeared and show no distinct trends, changes or peaks.

The component data (see section 2.2.) shows no obvious correlation between the corresponding units of the two cross-sections. This may be due to the nature of the distribution itself, although the restricted sample number may impede the detection of subtle underlying patterns.

### 5.2.1. Results based on Heavy Mineral Data

The results of a Factor Analysis (R-mode) on the data confirm the previous assumptions and reveal significant interrelationships. The heavy mineral data (Tab. 1) of 46 samples (units A, B, C, D, E, F and G in two cross-sections and along the ancient crater rim) were processed in Factor Analysis I.

The resulting correlation matrix shows a strong, negative correlation between the variables "olivine" and "pyroxene".

Almost 90 % of the total variances of variables "olivine", "pyroxene", "garnet" and "opaques" are taken into account by the four retained factors. The correlated variables "olivine", "pyroxene" and "weight percent" show high loadings in factor I, variables "hornblende", "garnet" and "opaques" each are dominant in the three remaining factors (Tab. 7).

In a second analysis (Factor Analysis II) the data were restricted (see section 5.1.) to the observations of units A, E, F and G (26 samples), and the significance of the variables within the three retained factors (explaining about 85 % of the total variance) was considerably increased. Variables "olivine" and "pyroxene" define factor III, "hornblende" factor II and "garnet" factor I (Tab. 8). More than 90 % of the variances of variables "olivine" and "pyroxene" and more than 88 % of the variance of variable "hornblende" are taken into account by the factors.

In regard to the given information, three dominating minerals (olivine, pyroxene, hornblende) seem to be very significant for the internal structure of the data set. The remaining variables lack important correlations

| Variable | Factor I | Factor II | Factor III | Factor IV |
|----------|----------|-----------|------------|-----------|
| OL | XX | – | – | – |
| HB | – | XXX | – | – |
| PY | XXX | – | – | – |
| GR | – | – | XXX | – |
| OT | – | – | – | – |
| OP | – | – | – | XXX |
| WT%HM | X | – | – | – |

Table 7.
Schematic factor matrix for Factor Analysis I (see Appendix C), showing the dominating variables for each rotated factor and the amount of variance that is taken into account.
OL = olivine; HB = hornblende; PY = pyroxene; GR = garnet; OT = others; OP = opaques; WT%HM = weight percent of heavy minerals per sample; XXX = > 80 % of variance; XX = >70 % of variance; X = > 50 % of variance.

| Variable | Factor I | Factor II | Factor III |
|----------|----------|-----------|------------|
| OL | – | – | X |
| HB | – | XX | – |
| PY | – | – | XXX |
| GR | X | – | – |
| OT | – | – | – |
| OP | – | X | – |
| WT%HM | X | – | – |

Table 8.
Schematic factor matrix for Factor Analysis II (see Appendix C), showing dominating variables for each rotated factor and and the amount of variance that is taken into account.
For legend see Tab. 7.

as well as genetic indications and may be eliminated from further statistical procedures.

### 5.2.2. Results Based on Heavy Mineral and Component Data

In Factor Analysis III, five factors were retained by processing the combined component analysis data (see section 3.3.; Tab. 3) of 28 consolidated samples and their corresponding heavy mineral data (Tab. 1, 2). The elimination of the observations of inconsistent beds (units B, C and D) increases the amount of variance of the significant variables taken into account by the factors. Due to the restricted component analysis data (see section 5.1.), only the observations of units A, F and G (20 samples) are processed in this analysis.

The factors group the variables according to their interrelationships. More than 90 % of the variances of the variables "olivine", "pyroxene", "hornblende", "matrix", "cryptocrystalline basalt clasts", "vitric basalt clasts" and more than 89 % the of variance of the variable "accretionary lapilli" is represented by the factors. These seven variables dominate factors I, II, IV and V, and they are thought to be most significant for the underlying structure of the data matrix. Factor III shows high loadings of the two slightly correlating variables "quartz/feldspar" and "volcanic lithics" (Tab. 9).

The number of factors retained and other differences between the results of the four analyses are due to the number of observations involved in the procedure. Changes concern only insignificant variables, while the dominating structures remain unaffected.

### 5.2.3. Interpretation

In regard to the information derived from the sequence of Factor Analyses and from field observations, the following interpretive statements may be made:

○ Variables "olivine" and "pyroxene" show a strong, negative correlation. The petrographically explained original interrelation may be amplified by induced correlation. However, a negative correlation between the abundance of olivine and pyroxene must reflect the crystallization processes of the two minerals, both containing considerable amounts of magnesium. Changes in the relative abundance of the minerals may also result from fractionation processes or differences of the magma source.

○ The variable "hornblende" has only a slight correlation to the two dominating minerals (Fig. 18), but may be a separate element in the structure of the data matrix.



(a)



(b)
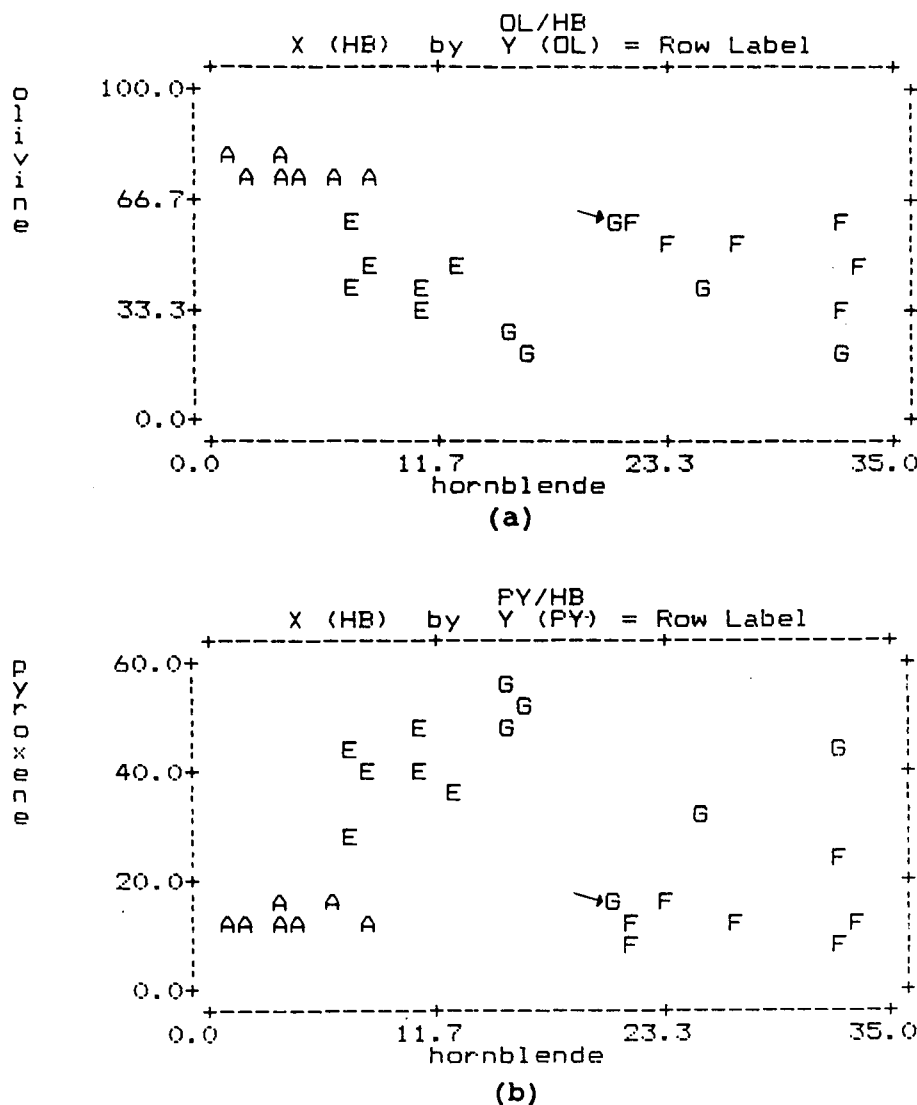
Fig. 18.
Scatter plots.
a) Hornblende grain % versus olivine grain %.
b) Hornblende grain % versus pyroxene grain %.
Symbols refer to original classification (see Tab. 10): A = unit A, E = unit E, F = unit F, G = unit G.
Sample S7 (marked by arrow), which was originally classified as surge deposit (unit G) but corrected and assigned to unit F (see section 5.3.1), clusters clearly with remaining samples of unit F. Samples with numerically close data values are represented with a single symbol (plot (a): samples A3 and A20, unit F; samples S9 and S10, unit G).

| Var. | FactorI | Factor II | Factor III | FactorIV | Factor V |
|------|---------|-----------|------------|----------|----------|
| OL | X | – | – | – | – |
| HB | – | – | – | XX | – |
| PY | XXX | – | – | – | – |
| GR | – | – | – | – | – |
| OT | – | – | – | – | – |
| OP | – | – | – | X | – |
| WT%HM | – | – | – | – | – |
| MAT | – | XX | – | – | – |
| CRY | – | XXX | – | – | – |
| VIT | – | – | – | – | XXX |
| QU | – | – | X | – | – |
| CLL | – | – | – | – | – |
| VOL | – | – | XX | – | – |
| CR | – | – | – | X | – |
| ACC | XX | – | – | – | – |
| VES | – | XX | – | – | – |

**Table 9.**
Schematic factor matrix for Factor Analysis IV (see Appendix C), showing dominant variables for each rotated factor and the amount of variance that is taken into account.
MAT = matrix; CRY = cryptocrystalline basalt clasts; VIT = vitric basalt clasts; QU = quartz and feldspar; CLL = clastic lithics; VOL = volcanic lithics; CR = crystals; ACC = accretionary and armored lapilli; VES = vesicles.
For legend see also Tab. 7.

○ The variables "garnet" and "others" (see section 2.1., Tab. 1 and 2) show no relation to obvious changes and events.

○ The expected negative correlation of variable "matrix" to variables "cryptocrystalline basalt clasts" and "vesicles" is partially induced by the closed system (see section 5.1.); still, these variables are used as descriptive factors in further procedures. Local high vesicularity of a few samples is thought to be due to physical processes too specific to be useful for a statistical classification.

○ Variables "volcanic lithics" and "clastic lithics" (see section 2.3. and Tab. 3) have an unproportionally large influence on the variance. This is induced by small values (0–3 counts per thin-section) and a frequent absence of those parameters.

○ Variables "quartz/feldspar" and "volcanic lithics" dominate one factor, and although their total variances are not significantly represented in the sum of the factors (communalities), the abundance of quartz and feldspar may be an additional element in the structure of the data matrix. Due to possible overweighting in the analysis, variable "volcanic lithics" may influence the results critically and is, therefore, not included in further procedures.

○ The strong, positive correlation between variables "pyroxene" and "accretionary lapilli" is the only significant interrelationship between heavy mineral data, which represent the mineralogical aspect, and component analysis data, which are thought to reflect physical processes during the eruption and the deposition of the material. The correlation is due to the fact that most of the material characterized by high amounts of pyroxene was deposited by wet pyroclastic surges which are likely to contain accretionary lapilli.

○ Variables "olivine", "pyroxene", "hornblende", "matrix", "cryptocrystalline basalt clasts", "vitric basalt clasts", "quartz/feldspar" and "accretionary lapilli" are significant for the underlying structure of the data set and are used in further statistical procedures.

○ The remaining variables may show inconsistent distribution patterns, which are not significantly related to stratigraphy and genetic processes. The related patterns may obscure the general structure under study and are, therefore, ignored in some of the consequent statistical procedures.

## 5.3. Discrimination and Classification

According to the stratigraphy and other field observations the samples have been classified prior to any statistical procedures (Tab. 10). Multivariate Discriminant Analysis is applied to test the significance of the deliberate classification as well as to assign samples of doubtful affiliation to one of the established groups (see section 5.1.).

The step-wise program (MDA) tends to eliminate the variable "olivine" because its variance is largely taken into account by the variable "pyroxene", to which it has a strong negative correlation. By reducing the heavy mineral variables to the three mineralogically most significant minerals (olivine, pyroxene and

| S. No. | unit | S. No. | unit | S. No. | unit |
|--------|------|--------|------|--------|------|
| A1* | F | A20 | F | A14F | A |
| A2 | F | A21 | F | | |
| A3* | F | A22 | F | A4A* | E |
| A5 | B | A23 | F | A4B* | E |
| A6H* | B | A25 | D | A4C* | E |
| A6L | B | A27 | D | A4D | E |
| A7 | B | A26 | C | A4E | E |
| A8 | B | A29 | B | A4F | E |
| A9H* | B | A30 | C | | |
| A9L | B | A31 | C | S5 | G |
| A10* | B | | | S6 | G |
| A11 | B | A14A | A | S7 | G |
| A12/4 | B | A14B* | A | S7(corr.) | F |
| A12/3* | B | A14C* | A | S8* | G |
| A12/2 | B | A14C1 | A | S9* | G |
| A12/1 | B | A14D | A | S10* | G |
| A13 | B | A14E | A | | |

**Table 10.**
Original sample classification based on stratigraphy and field observations.
* marks samples defining the original groups (dependent variables) for Multivariate Discriminant Analyses (see section 5.1.). Classification of sample S7 has been corrected from unit G to unit F.

| Analysis | F-value based on Wilk's Lambda | critical F-value | degrees of freedom |
|---|---|---|---|
| Analysis 1 | 159.00 | 2.20 | 8, 80 |
| Analysis 2 | 97.35 | 3.28 | 6, 21 |
| Analysis 3 | 43.06 | 3.83 | 4, 44 |
| Analysis 4 | 10.53 | 3.47 | 6, 30 |
| Analysis 5 | 13.02 | 3.09 | 10, 26 |
| Analysis 6 | - | - | - |
| Analysis 7 | 145.76 | 3.47 | 6, 30 |
| Analysis 8 | 34.65 | 3.47 | 6, 30 |
| Analysis 9 | 34.87 | 4.89 | 4, 15 |

Table 11.
Statistical tests on the significance of the separation of the groups and their relationship to the discriminant functions.
The results are significant if the F-value based on the distribution of Wilk's Lambda is larger than the critical F-value for i, j degrees of freedom. Level of significance is 1 %. The optimal Wilk's Lambda of 0.0000 in analysis 6 can not be transformed into the corresponding F-value (JOHNSON & WICHERN, 1988); but the original value of 0.0000 indicates high significance.

hornblende), it is possible to force the preferred variables into the process of establishing the discriminant function.

### 5.3.1. Results Based on Heavy Mineral Data

**Analysis 1**

Data of 46 samples were processed using a Multivariate Discriminant Analysis program, and the classification scheme described earlier was used for the dependent variable. The distribution of Wilk's Lambda

confirms the significance of the results on a level of 1 % (Tab. 11; for references see DAVIS, 1986, and JOHNSON & WICHERN, 1988). The variables "pyroxene" and "hornblende" (in order) were chosen for the formation of the discriminant functions. Lack of internal classification errors, significant separation of cluster means and high probabilities in the predicted classification (Tab. 12) indicate good predictability.

In regard to the original classification, based on field observations, several samples had been misclassified (A7, A8, A24, A29, A14E, A4D, S5 and S6; see Tab. 12). Most of these samples show some affinity to

| S.No. | Act | Pre | P(1) | P(2) | P(3) | P(4) | P(5) |
|---|---|---|---|---|---|---|---|
| A1 | 4 | 4 | 0.000 | 0.000 | 0.000 | 1.000 | 0.000 |
| A2 | | 4 | 0.000 | 0.000 | 0.000 | 1.000 | 0.000 |
| A3 | 4 | 4 | 0.000 | 0.003 | 0.000 | 0.997 | 0.000 |
| A5 | | 2 | 0.023 | 0.977 | 0.000 | 0.000 | 0.000 |
| A6H | 2 | 2 | 0.000 | 1.000 | 0.000 | 0.000 | 0.000 |
| A6L | | 2 | 0.000 | 0.908 | 0.000 | 0.092 | 0.000 |
| A7 | | 4 | 0.000 | 0.071 | 0.000 | 0.929 | 0.000 |
| A8 | | 4 | 0.000 | 0.336 | 0.000 | 0.664 | 0.000 |
| A9H | 2 | 2 | 0.000 | 1.000 | 0.000 | 0.000 | 0.000 |
| A9L | | 2 | 0.000 | 0.997 | 0.000 | 0.003 | 0.000 |
| A10 | 2 | 2 | 0.000 | 1.000 | 0.000 | 0.000 | 0.000 |
| A11 | | 2 | 0.000 | 1.000 | 0.000 | 0.000 | 0.000 |
| A12/4 | | 2 | 0.000 | 1.000 | 0.000 | 0.000 | 0.000 |
| A12/3 | 2 | 2 | 0.000 | 1.000 | 0.000 | 0.000 | 0.000 |
| A12/2 | | 2 | 0.000 | 1.000 | 0.000 | 0.000 | 0.000 |
| A12/1 | | 2 | 0.000 | 1.000 | 0.000 | 0.000 | 0.000 |
| A13 | | 2 | 0.000 | 1.000 | 0.000 | 0.000 | 0.000 |
| A20 | | 4 | 0.000 | 0.001 | 0.000 | 0.999 | 0.000 |
| A21 | | 4 | 0.000 | 0.000 | 0.000 | 1.000 | 0.000 |
| A22 | | 4 | 0.000 | 0.001 | 0.000 | 0.999 | 0.000 |
| A23 | | 4 | 0.000 | 0.000 | 0.000 | 1.000 | 0.000 |
| A25 | | 3 | 0.346 | 0.000 | 0.654 | 0.000 | 0.000 |
| A27 | | 4 | 0.000 | 0.000 | 0.000 | 1.000 | 0.000 |
| A26 | | 4 | 0.000 | 0.001 | 0.000 | 0.999 | 0.000 |
| A29 | | 1 | 0.771 | 0.229 | 0.000 | 0.000 | 0.000 |
| A30 | | 4 | 0.000 | 0.000 | 0.000 | 1.000 | 0.000 |
| A31 | | 4 | 0.000 | 0.003 | 0.000 | 0.997 | 0.000 |
| A14A | | 1 | 1.000 | 0.000 | 0.000 | 0.000 | 0.000 |
| A14B | 1 | 1 | 1.000 | 0.000 | 0.000 | 0.000 | 0.000 |
| A14C | 1 | 1 | 1.000 | 0.000 | 0.000 | 0.000 | 0.000 |
| A14C1 | 1 | 1 | 1.000 | 0.000 | 0.000 | 0.000 | 0.000 |
| A14D | 1 | 1 | 1.000 | 0.000 | 0.000 | 0.000 | 0.000 |
| A14E | | 2 | 0.384 | 0.616 | 0.000 | 0.000 | 0.000 |
| A14F | | 1 | 1.000 | 0.000 | 0.000 | 0.000 | 0.000 |
| A4A | 3 | 3 | 0.009 | 0.000 | 0.991 | 0.000 | 0.000 |
| A4B | 3 | 3 | 0.000 | 0.000 | 1.000 | 0.000 | 0.000 |
| A4C | 3 | 3 | 0.000 | 0.000 | 0.920 | 0.000 | 0.080 |
| A4D | | 5 | 0.000 | 0.000 | 0.004 | 0.000 | 0.996 |
| A4E | 3 | | 0.000 | 0.000 | 0.981 | 0.000 | 0.019 |
| A4F | | 5 | 0.000 | 0.000 | 0.029 | 0.000 | 0.971 |
| S5 | | 4 | 0.000 | 0.000 | 0.000 | 1.000 | 0.000 |
| S6 | | 4 | 0.000 | 0.046 | 0.000 | 0.954 | 0.000 |
| S7 | | 4 | 0.000 | 0.051 | 0.000 | 0.949 | 0.000 |
| S8 | 5 | 5 | 0.000 | 0.000 | 0.000 | 0.000 | 1.000 |
| S9 | 5 | 5 | 0.000 | 0.000 | 0.032 | 0.000 | 0.958 |
| S10 | 5 | 5 | 0.000 | 0.000 | 0.000 | 0.000 | 1.000 |

Table 12.
Predicted classification, analysis 1. S.No. = sample number; Act = actual (original) group number; Pred = predicted group number; P(i) = unbiased estimated probabilities that this sample belongs to group i (see Appendix C).
1 = pyroclastic flow deposit (unit A); 2 = epiclastic deposit (unit B); 3 = surge deposit I (unit E); 4 = lahar deposit (unit F); 5 = surge deposit II (unit G).

| S. No. | Act | Pred | P(1) | P(2) | P(3) | P(4) |
|--------|-----|------|------|------|------|------|
| A1 | 3 | 3 | 0.000 | 0.000 | 1.000 | 0.000 |
| A2 | | 3 | 0.000 | 0.000 | 1.000 | 0.000 |
| A3 | 3 | 3 | 0.000 | 0.000 | 1.000 | 0.000 |
| A20 | | 3 | 0.000 | 0.000 | 1.000 | 0.000 |
| A21 | | 3 | 0.000 | 0.000 | 1.000 | 0.000 |
| A22 | | 3 | 0.000 | 0.000 | 1.000 | 0.000 |
| A23 | | 3 | 0.000 | 0.000 | 1.000 | 0.000 |
| A14A | | 1 | 1.000 | 0.000 | 0.000 | 0.000 |
| A14B | 1 | 1 | 1.000 | 0.000 | 0.000 | 0.000 |
| A14C | 1 | 1 | 1.000 | 0.000 | 0.000 | 0.000 |
| A14C1 | | 1 | 1.000 | 0.000 | 0.000 | 0.000 |
| A14D | 1 | 1 | 1.000 | 0.000 | 0.000 | 0.000 |
| A14E | | 1 | 1.000 | 0.000 | 0.000 | 0.000 |
| A14F | | 1 | 1.000 | 0.000 | 0.000 | 0.000 |
| A4A | 2 | 2 | 0.030 | 0.970 | 0.000 | 0.000 |
| A4B | 2 | 2 | 0.001 | 0.997 | 0.000 | 0.002 |
| A4C | 2 | 2 | 0.000 | 0.898 | 0.000 | 0.102 |
| A4D | | 4 | 0.000 | 0.021 | 0.000 | 0.979 |
| A4E | 2 | | 0.000 | 0.951 | 0.000 | 0.049 |
| A4F | | 4 | 0.000 | 0.113 | 0.000 | 0.887 |
| S5 | | 3 | 0.000 | 0.000 | 1.000 | 0.000 |
| S6 | | 3 | 0.000 | 0.000 | 1.000 | 0.000 |
| S7 | | 3 | 0.000 | 0.000 | 1.000 | 0.000 |
| S8 | 4 | 4 | 0.000 | 0.001 | 0.000 | 0.999 |
| S9 | 4 | 4 | 0.000 | 0.061 | 0.000 | 0.939 |
| S10 | 4 | 4 | 0.000 | 0.000 | 0.000 | 1.000 |

**Table 13.**
Predicted classification, analysis 2. 1 = pyroclastic flow deposit (unit A); 2 = surge deposit I (unit E); 3 = lahar deposit (unit F); 4 = surge deposit II (unit G). For legend see also Tab. 12.

a second group, usually the original classification group. The samples of units C and D (A25, A26, A27, A30, A31) are preferably assigned to group 4, representing the lahar deposits. This preference may be enhanced by the considerable variance within this group, which consequently covers a large area in sample space. Samples that show no specific affinity and that can not form their own group are likely to be assigned to the group with the largest spread.

Sample S7 was originally thought to represent part of surge deposit II but is in all statistical procedures consistently classified as lahar deposit. According to its stratigraphic position it presumably does belong to unit F, which underlies the surge deposit.

## Analysis 2

Data of 26 samples (units A, E, F and G) were processed. On a significance level of 1 % the F-value based on Wilk's Lambda shows that the separation of the groups is significant (see Tab. 11). Again, variables „pyroxene" and "hornblende" (in order) were chosen for the linear discriminant functions and predictability is very high. Because of the reduced set of samples, the original classification is based on only 4 groups.

The groups representing pyroclastic flow and lahar deposits show no misclassifications with respect to field observations. The misclassifications of surge deposit samples correspond to the misclassifications in the previous analysis and may be caused by small mineralogical differences within the multilayered deposit or insufficient separations for a better result (Tab. 13).

## Analysis 3

The independent Cluster Analysis based on the K-means algorithm (26 samples; units A, E, F and G) indicates that 3 clusters take most of the variance into account. Variables "olivine", "hornblende" and

| S.No. | Act | Pred | P(1) | P(2) | P(3) |
|-------|-----|------|------|------|------|
| A1 | 2 | 2 | 0.000 | 0.999 | 0.000 |
| A2 | 2 | 2 | 0.000 | 1.000 | 0.000 |
| A3 | 2 | 2 | 0.017 | 0.983 | 0.000 |
| A20 | 2 | 2 | 0.012 | 0.988 | 0.000 |
| A21 | 2 | 2 | 0.000 | 1.000 | 0.000 |
| A22 | 2 | 2 | 0.009 | 0.991 | 0.000 |
| A23 | 2 | 2 | 0.001 | 0.999 | 0.000 |
| A14A | 1 | 1 | 1.000 | 0.000 | 0.000 |
| A14B | 1 | 1 | 1.000 | 0.000 | 0.000 |
| A14C | 1 | 1 | 1.000 | 0.000 | 0.000 |
| A14C1 | 1 | 1 | 0.999 | 0.001 | 0.000 |
| A14D | 1 | 1 | 0.998 | 0.002 | 0.000 |
| A14E | 1 | 1 | 0.990 | 0.010 | 0.000 |
| A14F | 1 | 1 | 0.801 | 0.002 | 0.197 |
| A4A | 3 | 3 | 0.009 | 0.000 | 0.991 |
| A4B | 3 | 3 | 0.002 | 0.000 | 0.998 |
| A4C | 3 | 3 | 0.000 | 0.000 | 1.000 |
| A4D | 3 | 3 | 0.001 | 0.000 | 0.999 |
| A4E | 3 | 3 | 0.000 | 0.000 | 1.000 |
| A4F | 3 | 3 | 0.000 | 0.000 | 1.000 |
| S5 | 3 | 3 | 0.001 | 0.118 | 0.881 |
| S6 | 3 | 3 | 0.000 | 0.000 | 1.000 |
| S7 | 2 | 2 | 0.031 | 0.969 | 0.000 |
| S8 | 3 | 3 | 0.000 | 0.000 | 1.000 |
| S9 | 3 | 3 | 0.000 | 0.000 | 1.000 |
| S10 | 3 | 3 | 0.000 | 0.000 | 1.000 |

**Table 14.**
Predicted classification, analysis 3. 1 = pyroclastic flow deposit (unit A); 2 = lahar deposit (unit F); 3 = surge deposit II (unit G). For legend see also Tab. 12.

| S.No | Act | Pred | P(1) | P(3) | P(4) |
|---|---|---|---|---|---|
| A1 | 3 | 3 | 0.024 | 0.924 | 0.051 |
| A2 | | 3 | 0.000 | 1.000 | 0.000 |
| A3 | 3 | 3 | 0.354 | 0.646 | 0.001 |
| A20 | | 1 | 0.981 | 0.019 | 0.000 |
| A21 | | 3 | 0.325 | 0.673 | 0.002 |
| A22 | | 3 | 0.152 | 0.846 | 0.003 |
| A23 | | 3 | 0.224 | 0.776 | 0.000 |
| A14A | | 1 | 0.986 | 0.014 | 0.000 |
| A14B | 1 | 1 | 0.873 | 0.124 | 0.003 |
| A14C | 1 | 1 | 0.978 | 0.021 | 0.000 |
| A14C1 | | 1 | 0.996 | 0.004 | 0.000 |
| A14D | 1 | 1 | 0.637 | 0.360 | 0.003 |
| A14E | | 3 | 0.224 | 0.776 | 0.000 |
| A14F | | 1 | 0.679 | 0.320 | 0.001 |
| S5 | | 1 | 0.989 | 0.010 | 0.001 |
| S6 | | 3 | 0.000 | 0.996 | 0.004 |
| S7 | | 1 | 0.916 | 0.084 | 0.000 |
| S8 | 4 | 4 | 0.120 | 0.113 | 0.766 |
| S9 | 4 | 4 | 0.000 | 0.000 | 1.000 |
| S10 | 4 | 4 | 0.001 | 0.051 | 0.948 |

**Table 15.**
Predicted classification, analysis 4.
For legend see Tab. 12. and 13.

"pyroxene" were processed to determine the cluster means, and the resulting classification groups were used for the dependent variable for the corresponding Multivariate Discriminant Analysis (Tab. 14).

Again, variables "pyroxene" and "hornblende" establish the linear discriminant functions. The distribution of Wilk's Lambda indicates that the results are significant (see Tab. 11).

The report (Tab. 14) shows the expected classification for all samples of pyroclastic flow deposit A and lahar deposit F. Both surge deposits are combined in group 3. This indicates that a further separation is not very efficient and that the heavy mineral distributions of the two surge deposits are similar.

### 5.3.2. Results Based on Component Data

#### Analysis 4

Analysis of component analysis data only yields rather poor results. The original groups are used for the classification variable and the step-wise program selected "accretionary lapilli", "quartz and feldspar clasts" and "cryptocrystalline basalt clasts" (in order) as independent variables. Variable "accretionary lapilli" is most significant for the discrimination and seems to be the only variable related directly to obvious physical processes during deposition. Variables "vitric basalt clasts" and "matrix" were rejected in the process of establishing the linear discriminant functions. The distribution of Wilk's Lambda shows that the results are still significant (see Tab. 11), although the predictability is considerably lower than in previous analyses.

In regard to field observations and earlier previous results, sample A20 (unit F) is misclassified as pyroclastic flow deposit and sample A14E (unit A) as lahar deposit, but both samples show affinity to their original group (Tab. 15). Group 4 (unit G) is poorly defined and shows no particular consistency in its component distribution. Due to lack of data, unit E (group 2) is not represented (see section 2.3.).

#### Analysis 5

An independent Cluster Analysis based on the distribution of components (see section 2.3.) classifies the samples of units A (pyroclastic flow deposit) and G (surge deposit II) with one misclassification each. The classification of the samples of the lahar deposits (unit F) is inconsistent.

The corresponding Multivariate Discriminant Analysis selects variables "volcanic lithics", "matrix", "crystals", "vesicles" and "clastic lithics" (in order) as independent variables. Wilk's Lambda indicates high predictability and good separation of the groups, but the classification and discrimination of the samples of unit F does not coincide with the original classification (see Tab. 16).

| S.No. | Act | Pred | P(1) | P(2) | P(3) |
|---|---|---|---|---|---|
| A1 | 3 | 3 | 0.000 | 0.000 | 1.000 |
| A2 | 3 | 3 | 0.000 | 0.000 | 1.000 |
| A3 | 1 | 1 | 0.997 | 0.003 | 0.000 |
| A20 | 2 | 2 | 0.001 | 0.999 | 0.000 |
| A21 | 1 | 1 | 0.845 | 0.155 | 0.000 |
| A22 | 2 | 1 | 0.843 | 0.157 | 0.000 |
| A23 | 1 | 1 | 0.813 | 0.187 | 0.000 |
| A14A | 2 | 2 | 0.002 | 0.998 | 0.000 |
| A14B | 2 | 2 | 0.030 | 0.970 | 0.000 |
| A14C | 2 | 2 | 0.000 | 1.000 | 0.000 |
| A14C1 | 2 | 2 | 0.006 | 0.994 | 0.000 |
| A14D | 2 | 2 | 0.008 | 0.992 | 0.000 |
| A14E | 2 | 2 | 0.093 | 0.907 | 0.000 |
| A14F | 1 | 1 | 0.944 | 0.056 | 0.000 |
| S5 | 1 | 1 | 0.981 | 0.019 | 0.000 |
| S6 | 1 | 1 | 1.000 | 0.000 | 0.000 |
| S7 | 1 | 1 | 0.994 | 0.006 | 0.000 |
| S8 | 2 | 2 | 0.154 | 0.846 | 0.000 |
| S9 | 1 | 1 | 0.993 | 0.007 | 0.000 |
| S10 | 1 | 1 | 0.976 | 0.024 | 0.000 |

**Table 16.**
Predicted classification, analysis 5.
1 = surge deposit II (unit G); 2 = pyroclastic flow deposit (unit A); 3 = lahar deposit (unit F).
For legend see also Tab. 12.

| S.No. | Act | Pred | P(1) | P(3) | P(4) |
|-------|-----|------|------|------|------|
| A1 | 3 | 3 | 0.000 | 1.000 | 0.000 |
| A2 | | 3 | 0.000 | 1.000 | 0.000 |
| A3 | 3 | 3 | 0.000 | 1.000 | 0.000 |
| A20 | | 3 | 0.000 | 1.000 | 0.000 |
| A21 | | 3 | 0.000 | 1.000 | 0.000 |
| A22 | | 3 | 0.000 | 1.000 | 0.000 |
| A23 | | 3 | 0.000 | 1.000 | 0.000 |
| A14A | | 1 | 1.000 | 0.000 | 0.000 |
| A14B | 1 | 1 | 1.000 | 0.000 | 0.000 |
| A14C | 1 | 1 | 1.000 | 0.000 | 0.000 |
| A14C1 | | 1 | 1.000 | 0.000 | 0.000 |
| A14D | 1 | 1 | 1.000 | 0.000 | 0.000 |
| A14E | | 1 | 1.000 | 0.000 | 0.000 |
| A14F | | 1 | 1.000 | 0.000 | 0.000 |
| S5 | | 1 | 1.000 | 0.000 | 0.000 |
| S6 | | 1 | 1.000 | 0.000 | 0.000 |
| S7 | | 3 | 0.000 | 1.000 | 0.000 |
| S8 | 4 | 4 | 0.000 | 0.000 | 1.000 |
| S9 | 4 | 4 | 0.000 | 0.000 | 1.000 |
| S10 | 4 | 4 | 0.000 | 0.000 | 1.000 |

Table 17.
Predicted classification, analysis 6.
For legend see Tab. 12. and 13.

Variable "accretionary lapilli", which is thought to be a good indicator for physical processes during deposition, is not taken in the discrimination function. This may be due to the influence of underlying structures based on the distribution patterns of other components that show no direct or clear relationship to depositional processes.

### 5.3.3. Results Based on Heavy Mineral and Component Data

#### Analysis 6

According to the underlying structures the variable set was restricted to variables "olivine", "hornblende", "pyroxene", "matrix", "cryptocrystalline basalt clasts", "vitric basalt clasts", "quartz and feldspar clasts" and "accretionary lapilli". The dependent variable is derived from the previously defined classification (see Tab. 10.). The independent variables selected by the step-wise program are (in order) "pyroxene", "hornblende", "vitric basalt clasts" and "cryptocrystalline basalt clasts". F-values based on Wilk's Lambda show that the results are highly significant (see Tab. 11). Very high probabilities for the predicted classification reflect the good separation of the 3 clusters but may also be amplified by the small number of samples.

Group 1 (pyroclastic flow deposits) and group 3 (lahar deposits) display perfect conformity with field observations. Two samples of unit G (pyroclastic surge deposit) show affinity to group 1 and are misclassified (Tab. 17).

#### Analysis 7

The elimination of variables "matrix", "cryptocrystalline basalt clasts", "vitric basalt clasts" and "quartz and feldspar clasts" and the deliberate acceptance of variable "accretionary lapilli" as selected independent variable do not alter the result significantly (Tab. 18). Therefore it is thought, that the discrimination is largely based on the distribution of the minerals pyroxene and hornblende.

#### Analysis 8

An independent Cluster Analysis groups the samples around cluster means, based on all observations of the involved sample pool. In regard to previous results the variable set was restricted to variables "olivine", "hornblende", "pyroxene" and "accretionary lapilli". The variation between the 3 clusters is not very high but still significant.

The clusters were used as classification variables in the corresponding Multivariate Discriminant Analysis. Variables selected for the discriminant function are (in order) "hornblende" and "pyroxene". Variable "accretionary lapilli" is included deliberately, although its

| S.No. | Act | Pred | P(1) | P(3) | P(4) |
|-------|-----|------|------|------|------|
| A1 | 3 | 3 | 0.000 | 1.000 | 0.000 |
| A2 | | 3 | 0.000 | 1.000 | 0.000 |
| A3 | 3 | 3 | 0.000 | 1.000 | 0.000 |
| A20 | | 3 | 0.000 | 1.000 | 0.000 |
| A21 | | 3 | 0.000 | 1.000 | 0.000 |
| A22 | | 3 | 0.000 | 1.000 | 0.000 |
| A23 | | 3 | 0.000 | 1.000 | 0.000 |
| A14A | | 1 | 1.000 | 0.000 | 0.000 |
| A14B | 1 | 1 | 1.000 | 0.000 | 0.000 |
| A14C | 1 | 1 | 1.000 | 0.000 | 0.000 |
| A14C1 | | 1 | 1.000 | 0.000 | 0.000 |
| A14D | 1 | 1 | 1.000 | 0.000 | 0.000 |
| A14E | | 1 | 1.000 | 0.000 | 0.000 |
| A14F | | 1 | 1.000 | 0.000 | 0.000 |
| S5 | | 3 | 0.405 | 0.595 | 0.000 |
| S6 | | 1 | 0.989 | 0.011 | 0.000 |
| S7 | | 3 | 0.000 | 1.000 | 0.000 |
| S8 | 4 | 4 | 0.000 | 0.000 | 1.000 |
| S9 | 4 | 4 | 0.000 | 0.000 | 1.000 |
| S10 | 4 | 4 | 0.000 | 0.000 | 1.000 |

Table 18.
Predicted classification, analysis 7.
For legend see Tab. 12. and 13.

| S.No. | Act | Pred | P(1) | P(2) | P(3) |
|-------|-----|------|-------|-------|-------|
| A1 | 1 | 1 | 0.998 | 0.000 | 0.002 |
| A2 | 1 | 1 | 1.000 | 0.000 | 0.000 |
| A3 | | 1 | 0.998 | 0.002 | 0.000 |
| A20 | 1 | 1 | 0.999 | 0.001 | 0.000 |
| A21 | 1 | 1 | 1.000 | 0.000 | 0.000 |
| A22 | 1 | 1 | 1.000 | 0.000 | 0.000 |
| A23 | 1 | 1 | 1.000 | 0.000 | 0.000 |
| A14A | 2 | 2 | 0.000 | 1.000 | 0.000 |
| A14B | 2 | 2 | 0.000 | 1.000 | 0.000 |
| A14C | 2 | 2 | 0.000 | 1.000 | 0.000 |
| A14C1 | 2 | 2 | 0.000 | 1.000 | 0.000 |
| A14D | 2 | 2 | 0.000 | 1.000 | 0.000 |
| A14E | 2 | 2 | 0.000 | 1.000 | 0.000 |
| A14F | 2 | 2 | 0.000 | 1.000 | 0.000 |
| S5 | 3 | 3 | 0.000 | 0.000 | 1.000 |
| S6 | 3 | 3 | 0.024 | 0.000 | 0.976 |
| S7 | 1 | 1 | 0.999 | 0.001 | 0.000 |
| S8 | 3 | 3 | 0.000 | 0.000 | 1.000 |
| S9 | 3 | 3 | 0.000 | 0.000 | 1.000 |
| S10 | 3 | 3 | 0.000 | 0.000 | 1.000 |

Table 19.
Predicted classification, analysis 8.
1 = lahar deposit (unit F); 2 = pyroclastic flow deposit (unit A); 3 = surge deposit II (unit G).
For legend see also Tab. 12.

F-probability value exceeds the critical value 0.1 (for references see DAVIS, 1986; BMDP (SOLO), 1989). The F-value based on Wilk's Lambda indicates that the results are highly significant (Tab. 11).

The grouping of the samples (Tab. 19) shows a distinct pattern that corresponds perfectly to the obvious stratigraphy and geological considerations. Note, that sample S7 is classified as lahar deposit (group 1).

Another set of analyses, where variables "pyroxene", "hornblende" and "vitric basalt clasts" establish the discriminant functions, misclassifies several samples and can not separate the lahar and the pyroclastic flow deposits. This indicates that careful restriction of the variable set – dependent on the objective of the study – has a strong influence on the results and may increase their significance considerably. Conversely, the process of selecting the variables allows fundamental conclusions on the importance of observations for a reasonable classification.

### Analysis 9

A more significant separation between the clusters is derived if only two groups are defined by an independent Cluster Analysis. The corresponding discriminant functions include all four variables ("olivine", "hornblende", "pyroxene" and "accretionary lapilli"), although only variable "pyroxene" meets the general demand for a F-probability value below 0.1 (for references see DAVIS, 1986; BMDP (SOLO), 1989). The distribution of Wilk's Lambda indicates high predictability, significant separation of the groups and good fit of the linear discrimination functions (Tab. 11).

However, the lahar deposits and pyroclastic flow deposits with similar distributions of heavy minerals and closely related depositional processes are combined in cluster 1 (note sample S7), while the significantly different surge deposits form group 2 (see Tab. 20).

### 5.3.4. Interpretation

The results of the classification-procedures applied on the volcaniclastic material near Beistein allow for the following interpretative statements:

● The deliberate classification based on field observations, statigraphy and geological assumptions is confirmed by independent Cluster Analyses, which group the samples in the same order. Due to the larger number of samples (and therefore observations) involved in the defining process of the cluster means, statistical clustering may, in some cases, even show a better grouping with respect to the original classification. Those units, that are represented by numerous samples and that are laterally consistent throughout the outcrop (units A, E, F and G), show the best separation.

Analysis 3 shows, that units E and G display a similar heavy mineral distribution, which reflects the

| S.No. | Act | Pred | P(1) | P(2) |
|-------|-----|------|-------|-------|
| A1 | 1 | 1 | 1.000 | 0.000 |
| A2 | 1 | 1 | 1.000 | 0.000 |
| A3 | 1 | 1 | 1.000 | 0.000 |
| A20 | 1 | 1 | 1.000 | 0.000 |
| A21 | 1 | 1 | 1.000 | 0.000 |
| A22 | 1 | 1 | 1.000 | 0.000 |
| A23 | 1 | 1 | 1.000 | 0.000 |
| A14A | 1 | 1 | 1.000 | 0.000 |
| A14B | 1 | 1 | 1.000 | 0.000 |
| A14C | 1 | 1 | 1.000 | 0.000 |
| A14C1 | 1 | 1 | 1.000 | 0.000 |
| A14D | 1 | 1 | 1.000 | 0.000 |
| A14E | 1 | 1 | 1.000 | 0.000 |
| A14F | 1 | 1 | 1.000 | 0.000 |
| S5 | 2 | 2 | 0.000 | 1.000 |
| S6 | 2 | 2 | 0.002 | 0.998 |
| S7 | 1 | 1 | 1.000 | 0.000 |
| S8 | 2 | 2 | 0.000 | 1.000 |
| S9 | 2 | 2 | 0.000 | 1.000 |
| S10 | 2 | 2 | 0.000 | 1.000 |

Table 20.
Predicted classification, analysis 9.
1 = lahar deposit (unit F) and pyroclastic flow deposit (unit A); 2 = surge deposit II (unit G).
For legend also see Tab. 12.

mutual source of their essential clasts and their common depositional processes. The absence of paleo-soil or major unconformities between the three uppermost units indicates, that both explosive events leading to the deposition of units E and G took place within a limited time interval. Mineralogical changes in the magma source are, therefore, expected to be very small.

Analysis 9 shows, that the statistical separation (based on available data) between unit A (pyroclastic flow deposit) and unit F (lahar deposit) is less significant than the difference between either and the surge deposit G. This is not surprising, if one considers, that lahar deposits are supposed to contain high amounts of reworked material. The voluminous pyroclastic flow deposit and the overlying epiclastic sediments containing high proportions of olivine are likely to have a significant impact on the heavy mineral spectrum of the lahar deposit (unit F). The thin surge deposit (unit E), presumably also incorporated into the overlying reworked deposit (unit F), may be too small for recognizable influences.

● Statistical separation of the distinct groups, that coincide with the different units, is largely based on the distribution of the dominant heavy minerals olivine, pyroxene and hornblende. Olivine and pyroxene are negatively correlated (see section 5.2.), therefore the distribution of pyroxene and hornblende is sufficient for a significant classification and discrimination.

The distribution of essential, accessory and accidental clasts poorly reflects the supposed variation between depositional processes. Discrimination based on the original classification and component analysis data is less significant for units A and F and fails to define a representative group for the samples of surge deposit II. The independent Cluster Analysis provides an acceptable classification of units A and G, but fails with unit F. It is obvious that useful structures of the distribution pattern do exist, but that they are not clear enough for a statistically significant separation of the expected stratigraphically defined groups. This may be a result of the complexity of physical processes that take place during deposition of volcaniclastic deposits. The depositional features (assumably represented in the distribution of clasts) depend on numerous external influences, that can not be recognized. Unknown processes or influences, that are not significant for the objective of the study, may manipulate the eventually resulting distribution or may cover up more significant but weak patterns.

The occurrence of accretionary or armored lapilli is the only variable with direct and exclusive relationship to the depositional processes. The rejection of the remaining variables of the component analysis and the deliberate acceptance of variable "accretionary lapilli" provides a highly significant result that confirms the original classification.

● The results indicate that multivariate processing based on the distribution of heavy mineral data provides a powerful tool in distinguishing several units within volcaniclastic successions. An essential assumption is, that changes of the heavy mineral spectra are significant enough for a statistical separation.

Additional information provided by the distribution patterns of a few selected clasts can improve the significance of the results. A higher number and a wider spread of samples over a larger area may weigh variables more accurately, and component data for classification and discrimination may become more important in classification and discrimination.

# 6. Conclusions

The volcaniclastic deposits near Beistein are the fragmental products of a maar volcanism that penetrated the Tertiary sediments of the Styrian Basin. Hydroclastic eruptions led to pyroclastic flow and pyroclastic surge deposits. The phreatomagmatic eruption style may have been dominant within the whole basaltic volcano field, which resumed activity at the end of Pliocene time. However, output of lava at nearby eruption centers additionally gave rise to scoria and basalt flow deposits.

Unpublished K/Ar data suggest an age of approximately 2 million years for the volcaniclastic deposits near Beistein (FLÜGEL & NEUBAUER, 1984). The formation may be subdivided into two major units:

1) Epiclastic and reworked material, including debris flow (lahar) deposits, fluvial deposits and lake deposits;

2) pyroclastic material, including surge, flow and air fall deposits.

The Tertiary sediments were overlain by a pyroclastic flow deposit (unit A) and locally by air fall deposits (unit C) and reworked material (units B, D), all derived from nearby eruption centers (Fig. 11 and 4.1.). The crater which is partially exposed at Beistein was formed by a phreatomagmatic eruption, that took place on the gentle slopes of the adjacent maar to the northwest. It was cut into the succession of clastic and volcaniclastic sediments. The maar-forming explosion produced a hot, dry base surge, which implies moderate water/magma ratios of 0.3 to 1.0 (SHERIDAN & WOHLETZ, 1981). The resulting deposit (unit E) contains highly fragmented material, which is densely packed due to the loss of superheated steam prior to emplacement.

Lahars overran the surge deposit shortly after deposition and incorporated loose, ashy material into the basal layer of their deposits. Additional debris flows, collapse of the inner crater walls, spalling and erosional processes formed a sequence of reworked material (A1 to A3, A20 to A23). Lateral variations of characteristics like thickness and texture within this unit (F) may be due to the local topographic position within the vent area.

Water derived from an aquifer or a newly formed crater lake triggered another eruption. Supply of abundant water (water/magma ratios >1; SHERIDAN & WOHLETZ, 1981) led to the formation of a sequence of predominantly wet surge deposits, which show bomb sag structures, occurrence of accretionary and armored lapilli and low-angle-cross-stratification. The eruption pulses produced single pyroclastic surges that travelled uphill on the inner sides of the crater rim. The dominating cross-stratified and interbedded massive beds exposed at Beistein represent the near-vent sandwave facies (WOHLETZ & SHERIDAN, 1979).

Volcanic activity ceased soon after at this eruption center. The crater was rapidly filled with lake sediments which are dominated by volcaniclastic layers. Bomb sag structures within the lake sediments give evidence for the proceeding volcanism nearby. A paleo-mud-boil indicates continuing high heat flow. Local post-basaltic pebble beds are the remnants of the final pre-glacial Quaternary deposit, and erosional processes, removing most of the edifice, formed the present relief and late volcaniclastic debris flows (Tab. 6).

The results of statistical analyses confirm the original classification of the major units exposed near Beistein (Fig. 11). The highly significant separation of the groups is largely based on the distribution of the dominant heavy minerals, olivine, hornblende and pyroxene. Amounts of olivine that exceed 70 grain percent characterize the deposits derived from the eruption center to the northwest of Beistein. Distinct peaks of pyroxene mark the surge deposits (E and G) that were produced by the events forming the Beistein crater. Due to the smearing effects of material mixing, the heavy mineral spectrum of the reworked deposit (F) is less distinct.

Distribution patterns of volcaniclastic clasts are thought to reflect the physical processes during deposition. Since these processes are specific for the resulting deposit, statistical tests based on component analysis data should be more profound than those dependent on the petrogenetic history.

The results of the statistical procedures, though, indicate that only the distribution of accretionary lapilli is significant for a reasonable classification and discrimination with respect to the geological background. Distribution patterns of the remaining components (see section 2.3.) seem to be too weak for a statistical separation. They also may be influenced or covered up by distribution structures that are not directly related to the major depositional processes. Furthermore, the physical processes of volcaniclastic deposits are very complex and, therefore, it may be difficult to recognize all influencing factors and their consequences.

A wider spread of samples over a larger area as well as higher sample numbers may help to overcome this problem. On this conditions the distribution of clasts alone may also be useful for a statistical classification and discrimination of volcaniclastic deposits.

The study shows, that statistical methods based on the distribution of heavy minerals provides a powerful tool to distinguish several units within volcanicalstic successions. An essential assumption is, that variations in the heavy mineral spectra are significant enough for a statistical separation. Additional information provided by the distribution patterns of a few selected clasts can improve the significance of the results.

## Glossary

**accidental clast:** Clasts derived from the subvolcanic basement of any composition.

**accretionary lapilli:** Lapilli, formed as aggregates of moist ash, commonly exhibiting a concentric internal structure.

**armored lapilli (= cored lapilli):** Lapilli-sized aggregate. An unstructured shell of ash covers a recognizable lithic core.

**ash:** Volcanic particles smaller than 2 mm.

**base surge:** Basal cloud moving rapidly outwards from a crater as a density flow. Frequently associated with phreatomagmatic eruptions.

**bomb:** Volcanic bomb. Volcanic ejecta, larger than 64 mm.

**cognate clasts (= accessory clasts):** Clasts of fragmented co-magmatic volcanic rocks from previous eruptions of the same volcano.

**cryptocrystalline:** Texture of a rock consisting of crystals that are to small to be recognized and distinguished under the ordinary microscope; indistinctly crystalline.

**diatreme:** Pipe-like volcanic conduit filled with pyroclastic debris and blocks of wallrock.

**ejecta:** Pyroclastic clasts, explosively ejected during a volcanic eruption.

**epiclastic:** Produced by weathering and erosion of consolidated volcanic rock.

**eruption:** One eruption is composed of several phases that may last a few days to months, or, in some basaltic volcanoes, for a few years.

**eruptive phase:** Volcanic event, that may last a few hours to days and consists of numerous eruptive pulses.

**eruptive pulse:** Volcanic event, that may last a few seconds to minutes.

**hydroclastic eruption (=hydromagmatic eruption):** Volcanic eruption' caused by interaction of magma and external water.

**juvenile:** (= essential). derived directly from the erupting magma, consisting of dense or inflated particles of chilled magma or pyrogenic crystals.

**lahar:** Debris flow of pyroclastic material on the flanks of volcanoes. Water is a major lubricant.

**lapilli:** Pyroclastics in the size range of 2 to 64 mm. lithics (= lithic fragments):
1) Slowly cooled and crystallized magma from chamber margins.
2) Rocks from the conduit walls.
3) Rock fragments picked up during transport.

**microcrystalline:** Texture of a rock concisting of crystals that are visible only under the microscope.

**phreatomagmatic eruption:** Explosion caused by interaction of ascending magma and external water. The resulting eruption products include juvenile, cognate and accidental ejecta. See also: hydroclastic eruption.

**pyroclastic:** Produced directly from volcanic processes.

**pyrogenic crystals:** Crystals that were present in the magma prior to eruption.

**volcaniclastic:** Volcanic and clastic, formed by a process of fragmentation, transported by any medium, emplaced in any environment, mixed in any proportion with nonvolcanic material.

**xenolith:** A foreign inclusion in an igneous rock.

# References

AGIORGITIS, G.: Zur Geochemie einiger seltener Elemente in basaltischen Gesteinen. – T. Min. Petr. Mitt., **12**, 204–229, Wien 1968.

AGIORGITIS, G.: Distribution of Iridium in some Basalts of South-eastern Central Europe. – T. Min. Petr. Mitt., **25**, 89–94, Wien 1978.

AGIORGITIS, G., SCHROLL, E. & STEPHAN, F.: K/Rb-, Ca/Sr- und K/Ti-Verhältnisse in basaltischen Gesteinen der Ostalpen und benachbarter Gebiete. – T. Min. Petr. Mitt., **14**, 285–309, Wien 1970.

ALKER, A., GOLOB, P., POSTL, P. & WALTINGER, H.: Neue Mineralfunde aus dem Nephelit des Stradner Kogels südlich Gleichenberg, Steiermark. – Mitt. Naturw. Ver. Stmk., **108**, 5–6, Graz 1978.

ALKER, A., GOLOB, P., POSTL, P. & WALTINGER, H.: Hydrotalkit, Nordstrandit und Motukoreait vom Stradner Kogel, südlich Gleichenberg, Steiermark. – Min. Mitt. Joanneum, **49**, 1–13, Graz 1981.

ARIC, K.: Deutung krustenseismischer und seismologischer Ergebnisse im Zusammenhang mit der Tektonik des Alpenostrandes. – Sitzungsber. Österr. Akad. Wiss., Math. Naturw. Kl., 1, **190**, 235–312, Wien 1982.

ARGUDEN, A.T. & RODOLFO, K.S.: Sedimentologic and dynamic differences between hot and cold laharic debris flows of Mayon Volcano, Phillipines. – Geol. Soc. Amer. Bull., **102**, 865–876, July 1990.

BATES, R.L. & JACKSON, J.A.: Dictionary of geological terms. – 571 p., New York London Toronto Sidney Auckland (Doubleday) 1984.

BENNET, F.D.: Shallow Submarine Volcanism. – J. Geophys. Res., **77**, 29, October 1972.

BERTOLDI, G.A., EBNER, F., HÖLLER, H. & KOLMER, H.: Blähton-vorkommen von Gnas und Fehring – geologische, sedimentpetrographische und technologische Untersuchungen. – Arch. Lagerstättenf. Geol. B.-A., **3**, 13–22, Wien 1983.

BOENIGK, W.: Schwermineralanalyse. – 77 Abb., 4 Taf., 8 Tab., 158 S., Stuttgart (Ferdinand Enke Publishers) 1983.

BMDP, STATISTICAL SOFTWARE INC.: User's Guide SOLO Statistical System Version 2.0. – Los Angeles California, August 1988.

CAS, R.A.F. & WRIGHT, J.V.: Volcanic Successions Modern and Ancient. – 528 p., London (Unwin Hynman) 1988.

CLAR, E.: Review of the structure of the Eastern Alps. – In: KEES, A., YOUNG, G. & SCHOTTEN, R.: Gravity and Tectonics, 235–270, London 1973.

CRANDELL, D.R.: Postglacial lahars from Mount Rainier volcano, Washington. – U.S. Geol. Survey Prof. Paper, **677**, 1–75, 1971.

CRANDELL, D.R. & WALDRON, H.H.: A recent volcanic mudflow of exceptional dimension from Mount Rainier, Washington. – Amer. J. Sci., **254**, 349–362, 1956.

DAVIS, J.C.: Statistics and Data Analysis in Geology. – 646 p., New York – Chichester – Brisbane – Toronto – Singapore (John Wiley & Sons) 1986.

EBNER, F., ERHART-SCHIPPEK, F. & WALACH, G.: Erdgasspeicher Oststeiermark. – Unpubl. Internbericht, Forschungsges. Joanneum, Institut f. Umweltgeologie u. Angew. Geographie, Graz 1985.

EBNER, F. & GRÄF, W.: Bericht über Literatur-, Gelände- und Laborarbeiten 1978 betreffend Tonvorkommen im Raum Fehring – Bad Gleichenberg – Gnas. – Unveröff. Bericht, 16 S., 3 Abb., Graz 1979.

FLÜGEL, H. & HERITSCH, H.: Das Steirische Tertiär-Becken. – Sammlg. Geol. Führer, **47**, 196 S., 27 Abb., 8 Taf., 1 geol. Karte, Berlin – Stuttgart (Gebr. Borntraeger) 1968.

FLÜGEL, H.W. & NEUBAUER, F.: Steiermark Erläuterungen zur Geologischen Karte der Steiermark 1 : 200.000. – 127 S., Wien (Geologische Bundesanstalt) 1984.

FISHER, R.V. & SCHMINCKE, H. – U.: Pyroclastic Rocks. – 471 p., Berlin – Heidelberg – New York – Tokyo (Springer) 1984.

FISHER, R.V. & WATERS, A.C.: Base Surge Bed Forms in Maar Volcanoes. – Amer. J. Sci., **268**, 157–180, February 1970.

FOLK, R.L.: Petrology of sedimentary rocks. – Austin (Hemphill) 1980.

FRANCIS, E.H.: Magma and sediment–II. Problems of interpreting palaeovolcanics buried in the stratigraphic column. – J. Geol. Soc. Lond., **140**, 165–83, London 1983.

HERITSCH, H.: Gismondit aus dem Nephelinit des Stradner Kogels bei Gleichenberg, Steiermark. – Anz. Österr. Akad. Wiss., math.-naturw. Kl., **1963**, 153–154, Wien 1963.

HERITSCH, H.: Über Einschlüsse im Basanit von Klöch, Oststeiermark. – Anz. Österr. Akad. Wiss., math.-naturw. Kl., **1964**, 247–248, Wien 1964.

HERITSCH, H.: Das oststeirische Vulkangebiet. – Fortschr. Min., **42**, 165–169, Stuttgart 1965.

HERITSCH, H.: Vulkanische Gesteine vom Steinberg bei Feldbach. – Mitt. Naturw. Ver. Stmk., **98**, 16–26, Graz 1968a.

HERITSCH, H.: Drei seltene Silikate aus dem Basanitsteinbruch von Klöch, Südost-Steiermark. – Anz. Österr. Akad. Wiss., math.-naturw. Kl., **1968**, 177–178, Wien 1968b.

HERITSCH, H.: Ni-Gehalte von Olivinen aus Olivinbomben und basaltischen Gesteinen des oststeirischen Vulkanbogens. – Anz. Österr. Akad. Wiss., math.-naturw. Kl., **1970**, 10–12, Wien 1969.

HERITSCH, H.: Über mögliche Beziehungen zwischen den Haupttypen des pliozänen, basaltischen Vulkanismus der Oststeiermark. – Anz. Österr. Akad. Wiss., math.-naturw. Kl., **1975**, 147–152, Wien 1975.

HERITSCH, H.: Über Nephilinbasanite und ein basaltisches Glas des Vulkangebietes von Klöch, Oststeiermark. – Mitt. Naturw. Ver. Stmk., **106**, 21–29, Graz 1976a.

HERITSCH, H.: Ein Vergleich glasiger Grundmassen und selbständiger Gläser des pliozänen Vulkanismus der Oststeiermark. – Anz. Österr. Akad. Wiss., math.-naturw. Kl., **1976**, 163–165, Wien 1976b.

HERITSCH, H., BERTHOLDI, G. & WALITZI, E.M.: Strukturuntersuchungen an einer basaltischen Hornblende vom Kurizzenkogel südlich Fehring, Steiermark. – T. Min. Petr. Mitt., (III. Folge), **7**, 210–217, Wien 1960.

HERITSCH, H. & HÖLLER, H.: Tertiär, Vulkanismus und Randgebiete der südlichen Steiermark (Weitendorf, Steinbruch Klause bei Gleichenberg, Bad Gleichenberg, Feldbacher Steinberg, Kapfenstein, Steinbruch Fürbas, Steinofen Hohl, Steinbruch Prettner bei Gams). – Mitt. Geol. Ges. Wien, **63**, 275–289, Wien 1970.

HERITSCH, H. & HÜLLER, H.J.: Über die Entstehung von Basaltgläsern in basaltischen Gesteinen des Steinberges bei Feldbach, Steiermark, Österreich. – T. Min. Petr. Mitt., **20**, 73–80, Wien 1973.

HERITSCH,H. & HÜLLER, H.J.: Chemische Analysen von basaltischen Gesteinen und Gläsern, sowie von Nephelin aus dem Westbruch des Steinberges bei Feldbach, Oststeiermark. – Mitt. Naturw. Ver. Stmk., **105**, 43–52, Graz 1975.

HERITSCH H. & ROHANI, H.: Untersuchungen über Olivin und Klinopyroxen sowie über Auswürflinge des basaltischen Vulkanismus der Oststeiermark. – Mitt. Naturw. Ver. Stmk., **103**, 7–22, Graz 1973.

HERMANN, O.: Sekundäre Veränderungen an Lapilli aus Tuffiten des Oststeirischen Vulkangebietes. – Anz. Österr. Akad. Wiss., math.-naturw. Kl., **1974**, 96–102, Wien 1974.

HESS, P.C.: Origins of igneous rocks. – 336 p., Cambridge London (Harvard University Press) 1989.

HÖLLER, H.: Untersuchungen an vulkanischen Tuffen bei Eibiswald. – Min. Mitt. Joanneum, 1961, 54–56, Graz 1961.

HÖLLER, H.: Über Zeolithbildung in zersetzten vulkanischen Gesteinen und Tuffen der Steiermark. – Anz. Österr. Akad. Wiss., math.-naturw. Kl., **1965**, 320–323, Wien 1965.

HÖLLER, H.: Blähtonvorkommen von Gnas. – Steir. Beitr. Rohstoff. Energief., **2**, 14–16, Graz 1982.

HÖLLER,H., KOLMER, H. & WIRSCHING, U.: Chemische Untersuchungen der Umwandlung glasiger Tuffe in Montmorilonit- und Kaolinit-Minerale. – N. Jb. Min. Mh., **1976**, 456–466, Stuttgart 1976.

HORVATH, F. & BERCKHEMER, H.: Mediterranean Backarc Basins. – In: BERCKHEMER & HSÜ (Eds.): Alpine-Mediterranean Geodynamics Geodynamics Series, 7, 141–174, (American Geophysical Union) 1982.

HÜLLER, H.J.: Petrographische Untersuchungen über die Entstehung von Basaltgläsern in basaltischen Gesteinen des Steinberges bei Feldbach (Steiermark, Österreich). – Diss. Univ. Graz, 97 S., Graz 1974.

INMAN, D.L.: Measures for describing the size distribution of sediments. – J. Sed. Petrol., **22**, 125–45, 1952.

JOHNSON, A.J., WICHERN, D.W.: Applied Multivariate Statistical Analysis. – 2nd edition, 594 p., Englewood Cliffs, New Jersey (Prentice-Hall, Inc.) 1988.

KIENLE, J., KYLE, P.R., SELF, S., MOTYKA, R.J. & LORENZ, V.: Ukinrek Maars, Alaska, I. April 1977 Eruption Sequence, Petrology and Tectonic Setting. – J. Volc. Geotherm. Res., 7, 11–37, Amsterdam (Elsevier Science Publishers B.V.) 1980.

KAURAT, G.: Granat-, Spinell-, Websterit- und Lherzolit aus dem Basalttuff von Kapfenstein, Steiermark. – T. Min. Petr. Mitt., **16**, 192–214, Wien 1971.

KAURAT, G., KRACHER, A., SCHARBERT, H.G.: Petrologie des oberen Erdmantels unterhalb von Kapfenstein, Steiermark. – Fortschr. Miner., **54**, 53–54, Stuttgart 1976.

KAURAT, G., PALME, H. & SPETTEL, B.: Geochemistry of the Mantle under Kapfenstein, Styria (Xenoliths from Basalt). – Fortschr. Miner., **55**, 142–143, Stuttgart 1977.

KAURAT, G., PALME, H., SPETTEL, B., BADDENHAUSEN, H., HOFMEISTER, H., PALME, Ch. & WÄNKE, H.: Geochemistry of ultramafic xenoliths from Kapfenstein, Austria: Evidence for a variety of upper mantle processes. – Geochim. Cosmochim. Acta, **44**, Oxford 1980.

LAJOIE, J.: Facies models 15. Volcaniclastic rocks. – Geoscience Can. 6, no.3, 129–139, Kitchener Ontario 1979.

LEWIS, D.W.: Practical Sedimentology. – 229 p., Stroudsburg, Pennsylvenia 1984.

LORENZ, V.: On the growth of maars and diatremes and its relevance to the formation of tuff rings. – Bull. Volc., **48**, 265–274, (Springer) 1986.

LORENZ, V.: Studies of the Surtsey tephra deposits. – Reprint from Surtsey Research Progress Report VII, 72–79, 1974.

MEISSNER, R. & STEGENA, L.: Lithosphere and Evolution of the Pannonian Basin. – In: ROYDEN & HORVATH (Eds.): The Pannonian Basin. A Study In Basin Evolution. – AAPG Memoir, **45**, 147–152, Tulsa Oklahoma (AAPG) 1988.

OFFENBACHER, H.: Die Mineralien des Nephelinbasanit-Steinbruches von Klöch. – Die Eisenblüte, **4**, 1–6, Graz 1979.

PAULITSCH, P.: Thaumasit im Basalt von Klöch, Steiermark. – Aufschluss, **24**, 266–268, Heidelberg 1973.

POKA, T.: Neogene and Quarternary Volcanism of the Carpathian-Pannonian Region: Changes in Chemical Composition and Its Relationship to Basin Formation. – In: ROYDEN & HORVATH (Eds.): The Pannonian Basin. A Study In Basin Evolution. – AAPG Memoir, **45**, 257–278, Tulsa Oklahoma (AAPG) 1988.

PÖSCHL, I.: Bericht 1989 über geologische Aufnahmen des Gebietes um Beistein auf Blatt 192 Feldbach. – Jb. Geol. B.-A., **133/3**, 499, Wien 1990.

POSTL, W. & WALTER, F.: Ettringit und Thaumasit aus dem Nephelinbasanit von Klöch, Steiermark. – Mitt. Abt. Miner. Joanneum, **51**, 33–36, Graz 1983.

POULTIDES, Ch.: Petrologie und Geochemie basaltischer Gesteine des steierischen Vulkanbogens in der Steiermark und im Burgenland. – Diss. Univ. Wien, 146 S., Wien 1981.

REINECK, H.-E. & SINGH, I.B.: Depositional Sedimentary Environments (with reference to terrigenous clastics). – 549 p., 683 fig., Berlin – Heidelberg – New York (Springer) 1980.

ROYDEN, L.H.: Late Cenozoic Tectonics of the Pannonian Basin System. – In: ROYDEN & HORVATH (Eds.): The Pannonian Basin. A Study In Basin Evolution. – AAPG Memoir, **45**, 27–47, Tulsa Oklahoma (AAPG) 1988.

SCHARBERT, H.G.: The Earth's upper mantle below Kapfenstein (eastern Styria, Austria). – Min. Soc. Bull., **34**, 6, London 1977.

SCHARBERT, H.G., POULTIDES, CH., HÖLLER, H., KOLMER, H. & WIRSCHING, U.: Vulkanite im Raume Burgenland – Oststeiermark. – Fortschr. Miner., **59**, 69–88, Stuttgart 1981.

SCLATER, J.G., ROYDEN, L., HORVATH, F., BURCHFIEL, B.C., SEMKEN, S. & STEGENA, L.: The Formation Of The Intra-carpathian Basins As Determined From Subsidence Data. – Earth and Planetary Science Letters, **51**, 139–162, Amsterdam (Elsevier Scientific Publishing Company) 1980.

SCHMID, R.: Descriptive nomenclature and classification of pyroclastic deposits and fragments: Recommendations of the IUGS Subcommission on the Systematics of Igneous Rocks. – Geology, **9**, 41–43, January 1981.

SELF, S., KIENLE, J. & HUOT, J.-P.: Ukinrek Maars, Alaska, II. Deposits and Formation of the 1977 Craters. – J. Volc. Geotherm. Res., **7**, 39–65, Amsterdam (Elsevier) 1980.

SHERIDAN, M.F.: Emplacement of pyroclastic flows: A review. – Geol. Soc. Amer., Spec. Paper **180**, 125–136, 1979.

SHERIDAN, M.F. & WOHLETZ, K.H.: Hydrovolcanic Explosions. The systematics of water-pyroclast equilibration. – Science, **212**, 1387–1389, 1981.

SPARKS, R.S.J.: Grain size variations in ignimbrites and implications for the transport of pyroclastic flows. – Sedimentology, **23**, 147–188, 1976.

SPARKS, R.S.J., WILSON, L. & HULME, G.: Theoretical modelling of the generation, movement and emplacement of pyroclastic flows by column collapse. – J. Geoph. Res., **83**, 1727–1739, 1978.

SMITH, G.A.: Coarse-grained nonmarine volcaniclastic sediment: Terminology and depositional process. – Geol. Soc. Amer. Bull., **97**, 1–10, 6 figs., 1 tab., January 1986.

VESSELL, R.K. & DAVIES, D.K.: Non-marine sedimentation in an active fore-arc basin. – In: , F.G. ETHRIDGE & R.M. FLORES (Eds.): Recent and ancient non-marine depositional environments: models for exploration. – SEPM Spec. Publ. **31**, 31–45, 1981.

VETTERS, W.: Zur Genese des Tuffes von Pertlstein bei Feldbach (Steiermark). – Karinthin, **76**, 287–289, Salzburg 1977.

VOGELHUBER, W. & WEIGEL, J.: Das Illitvorkommen bei Fehring, Oststeiermark. – Montan. Rdsch., **9**, 187–190, Wien 1961.

WALKER, G.P.L.: Characteristics of Dune-Bedded Pyroclastic Surge Bedsets. – J. Volc. Geotherm. Res., **20**, 281–296, Amsterdam (Elsevier Science Publishers B.V.) 1984.

WALKER, G.P.L.: Explosive volcanic eruptions–a new classification scheme. – Geol. Rundsch., **62**, 431–446, 1973.

WATERS, A.C. & FISHER, R.V.: Base surges and their deposits: Caphelinos and Taal volcanoes. – J. Geophys. Res., **76**, 5596–5614, 1971.

WIEDEN, P. & SCHMIDT, J.: Der Illit von Fehring. – Tschermaks Min. Petr. Mitt., **5**, 284–302, 1956.

WILSON, L., PINKERTON, H. & MACDONALD, R.: Physical Processes In Volcanic Eruptions. – Ann. Rev. Earth Planet. Sci., **15**, 73–95, 1987.

WINKLER-HERMADEN, A.: Erläuterungen zur geologischen Spezialkarte der Republik Österreich, Blatt Marburg. – 68 S., Wien 1938.

WINKLER-HERMADEN, A.: Geologischer Führer durch das Tertiär- und Vulkanland des Steirischen Beckens. – Sammlg. Geol. Führer, **36**, 209 S., 27 Abb., 3 Taf., Berlin (Borntraeger) 1939.

WINKLER-HERMADEN, A.: Geologisches Kräftespiel und Landformung. – 822 p., Wien (Springer) 1957.

WOHLETZ, K.H. & SHERIDAN, M.F.: A model of pyroclastic surge. – Geol. Soc. Amer., Spec. Paper **180**, 177–194, 1979.

WOHLETZ, K.H., SHERIDAN, M.F.: Hydroclastic Explosions II. Evolution of Basaltic Tuff Rings and Tuff Cones. – Amer. J. Sci., **283**, 385–413, 1983.

# ZOBODAT - www.zobodat.at